

Low-Cost High-Power Membership Inference Attacks

Sajjad Zarifzadeh, Philippe Liu and Reza Shokri
National University of Singapore

Abstract

Membership inference attacks (MIA) aim to detect if a particular data point was used in training a machine learning model. Recent strong attacks have high computational costs and inconsistent performance under varying conditions, rendering them unreliable for practical privacy risk assessment. We design a novel, efficient, and robust membership inference attack (RMIA) which accurately differentiates between population data and training data of a model, with minimal computational overhead. We achieve this by a more accurate modeling of the null hypothesis setting in our likelihood ratio tests, and effectively leveraging both reference models and reference data samples from the population. Our algorithm exhibits superior test power (true-positive rate) compared to prior methods, throughout the TPR-FPR curve including at extremely low false-positive rates (as low as 0). Under computation constraints, where only a limited number of pre-trained reference models (as few as 1) are available, and also when we vary other elements of the attack, our method performs exceptionally well, unlike some prior attacks that approach random guessing. RMIA outperforms the prior work in all configurations of the attack setup. RMIA lays the algorithmic groundwork for practical yet accurate and reliable privacy risk analysis in machine learning.

1 Introduction

Membership inference attacks are used to quantify the information leakage of machine learning algorithms about their training data [43]. Membership inference attacks originated within the realm of summary statistics on high-dimensional data [20]. In this context, different hypothesis testing methods were designed to optimize the trade-off between test power and its error [42, 49, 15, 35]. For deep learning algorithms, these tests evolved from using ML itself to perform the membership inference [43] to using various approximations of the original statistical tests [40, 54, 8, 51, 4]. Attacks also vary based on the threat models and the computation needed to tailor the attacks to specific data points and models (e.g., global attacks [43, 56] versus per-sample tailored attacks [54, 8, 40, 51]) which necessitate training a *large* number of reference models to achieve a high test power.

Although there have been improvements in the effectiveness of attacks, their **computation cost** renders them useless for practical privacy auditing. Also, as it is shown in the prior work the the SOTA attacks [8, 54] exhibit mutual dominance *depending on the test scenarios!* In the abundance of computation budget [54] shows low power at low FPR, and with practical computation budget, [8] verges on **random guessing**. Through extensive empirical analysis, we observe further **performance instabilities** in the prior SOTA attacks across different settings, where we investigate the impact of varying the number of reference models, the number of required inference queries, the similarity of reference models to the target model, the distribution shift in target data versus population data, etc. This calls for *more robust and reliable yet efficient* inference attacks.

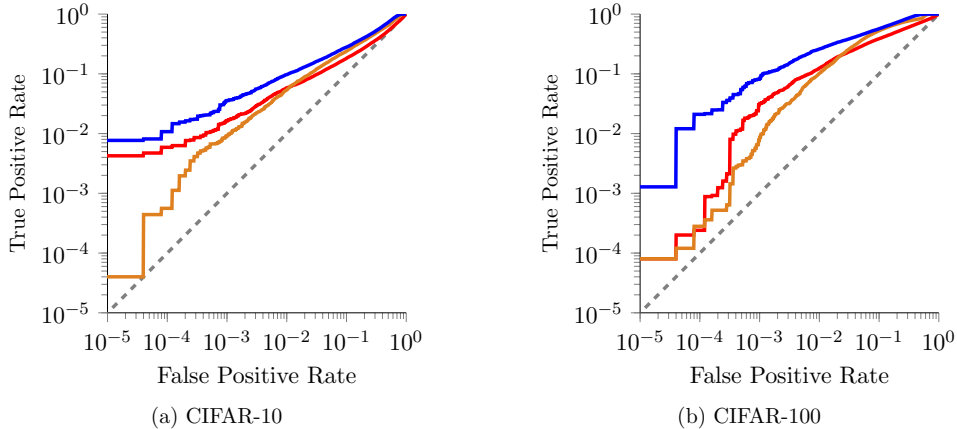


Figure 1: Performance of RMIA versus the SOTA prior attacks (Attack-R [54] and LiRA [8]), under computation constraints, with the restriction of using only 1 reference model, in an offline setting. RMIA outperforms other attacks throughout the TPR-FPR trade-off curve. Note the AUC that LiRA approaches random guessing.

Membership inference attack is a hypothesis testing problem. Attacks are evaluated based on their TPR-FPR curve on benchmark models. We design a **novel membership inference test** by enumerating the fine-grained plausible worlds associated with the null hypothesis, in which the *target data point could have been replaced with any random sample from the population*. We perform the attack by composing the likelihood ratio (LR) tests of these cases. Our test enhances the differentiation between member and non-member data points, enabling a more precise estimation of test statistics. The computation we propose to compute the LR test statistics is also very stable and extremely efficient (as it requires very few reference models). **Our robust attack method RMIA dominates prior work in all test scenarios, and consistently achieves a high TPR across all FPR (even as low as 0), given any computation budget.** Another significant aspect of our framework is that many *prior attacks can be framed as simplifications of ours*. Our interpretation reveals the implicit assumptions and simplifications in prior methods, shedding light on their reduced performance and instability.

In our empirical analysis, we show that RMIA outperforms prior SOTA attacks across benchmark datasets, by achieving 5 – 10% higher AUC and a significant $2\times$ to $4\times$ higher TPR at low FPRs, when using only 2 reference models. When considering just 1 single reference model, the improvement is significant. See Figure 1. When dealing with a few reference models, [54] mainly suffers from low TPR at low FPR, while [8] fails to even get an AUC score beyond random guessing. In an offline scenario, where the adversary exclusively uses pre-trained reference models, RMIA demonstrates an impressive 28% higher AUC and $3\times$ better TPR at **zero FPR**. Also, the offline version of our attack shows a comparable performance to online attacks. Designing online MIA—where a large number of new reference models are required for each and every membership query—renders attacks with low FPR impractical. This is because the advantage of having a low FPR primarily comes into play when the attack is evaluated using a large number of non-member (potentially OOD) data. Beyond varying the computation budget of the attack, we test how shifting the distribution of training data and population data (by using noisy and OOD data), and modifying model architectures, can impact the attack performance. We perform extensive evaluations, and even when considering worst-case scenarios,

RMIA consistently outperforms prior attacks in all settings.

2 Performing Membership Inference Attacks

Membership inference attacks (MIA) determine whether a specific data point x was used in the training of a given machine learning model θ . MIA is defined by an indistinguishability game between a challenger and adversary (i.e., privacy auditor) [56]. See [54] for a comprehensive presentation of MIA games. We use the widely-used game and attack template [20, 42, 56, 8, 54, 4]. The game models random experiments related to two hypotheses: 1. the model θ was trained using x , and 2. x was not in θ 's training set (the null hypothesis). The adversary is randomly placed in one of these two worlds and tasked with inferring which world he is in, using only data point x , the trained model θ , and his background knowledge about the training algorithm and population data distribution.

Definition 2.1 (Membership Inference Game) *Let π be the data distribution, and let \mathcal{T} be the training algorithm.*

- i – The challenger samples a training dataset $S \sim \pi$, and trains a model $\theta \sim \mathcal{T}(S)$.*
- ii – The challenger flips a fair coin b . If $b = 1$, it randomly samples a data point x from S . Otherwise, it samples $x \sim \pi$, such that $x \notin S$. The challenger sends the target model θ and the target data point x to the adversary.*
- iii – The adversary, having access to the distribution over the population data π , computes $\text{Score}_{\text{MIA}}(x; \theta)$ and uses it to output a membership prediction bit $\hat{b} \leftarrow \text{MIA}(x; \theta)$.*

A membership inference attack assigns a membership score $\text{Score}_{\text{MIA}}(x; \theta)$ to every pair of (x, θ) , and performs the hypothesis testing by outputting a membership bit through comparing the score with a threshold β :

$$\text{MIA}(x; \theta) = \mathbb{1}_{\text{Score}_{\text{MIA}}(x; \theta) \geq \beta} \quad (1)$$

The adversary's **power** (true positive rate) and **error** (false positive rate) are quantified over numerous repetitions of the MIA game experiment. The threshold β controls the error the adversary is willing to tolerate [42, 54, 4].

The $\text{Score}_{\text{MIA}}(x; \theta)$ and the test equation 1 are designed to maximize the **MIA test performance** as its power (TPR) for any FPR. The (lower-bound for the) *leakage* of the ML algorithm is defined as the power-error trade-off curve (the ROC curve), which is derived from the outcome of the game experiments across all values of β . We consider the **efficiency and stability** of the MIA test as critical criteria for reliable and practical privacy auditing.

3 Designing RMIA

We design RMIA by constructing a novel test for membership inference attacks. We compose the null hypothesis (where x is not a member of the training set of θ) as the worlds in which the target data point x is replaced with a random data point z sampled from the population. Thus, we design many **pairwise likelihood ratio tests** to test the membership of a data point x *relative* to another data point z . To reject the null hypothesis, we need to collect substantial evidence (i.e., numerous instances of population data z) that the probability of observing θ under the hypothesis that x is in its training set is larger than the probability of observing θ when instead a random z is in the training set. This approach provides a much more fine-grained

analysis of leakage, and differentiates between the worlds in which x is not a member (as opposed to relying on the average likelihood of the null hypothesis). The likelihood ratio corresponding to the pair of x and z is:

$$\text{LR}_\theta(x, z) = \frac{\Pr(\theta|x)}{\Pr(\theta|z)}, \quad (2)$$

where $\Pr(\theta|\cdot)$ is computed over the randomness of the training algorithm (e.g., SGD). The term $\Pr(\theta|x)$ is the probability that the algorithm produces the model θ given that x was in the training set, while the rest of the training set is randomly sampled from the population distribution π .

Computing the Likelihood Ratio. To efficiently compute the pair-wise LR values in the black-box setting (where the adversary can observe the model output), we apply the Bayes rule to compute equation 2:¹

$$\text{LR}_\theta(x, z) = \left(\frac{\Pr(x|\theta)}{\Pr(x)} \right) \cdot \left(\frac{\Pr(z|\theta)}{\Pr(z)} \right)^{-1} \quad (3)$$

Here, $\Pr(x|\theta)$ is the likelihood function of model θ evaluated on data point x . In the case of classification models, and black-box MIA setting, $\Pr(x|\theta)$ is the prediction score (SoftMax) of output of the model $f_\theta(x_{\text{features}})$ for class x_{label} [33, 5].²

It is important to note that $\Pr(x)$ is not the same as $\pi(x)$, which is rather the prior distribution over x . The term $\Pr(x)$ is the normalizing constant in the Bayes rule, and is computed by integrating over all models θ' with the same structure and training data distribution as θ .

$$\Pr(x) = \sum_{\theta'} \Pr(x|\theta') \Pr(\theta') = \sum_{D, \theta'} \Pr(x|\theta') \Pr(\theta'|D) \Pr(D) \quad (4)$$

We compute $\Pr(x)$ as the empirical mean of $\Pr(x|\theta')$ by sampling *reference models* θ' , each trained on random datasets D drawn from the population distribution π . When computing this empirically, we need to make sure the reference models are sampled in an *unbiased* way with respect to whether x is part of their training data D . See Appendix B.2.2, for the details of computing unbiased $\Pr(x)$ from reference models in both online and offline attack settings. The same computation process applies to $\Pr(z)$.

Constructing RMIA by Composing Pair-Wise LRs. Given $\text{LR}_\theta(x, z)$, we formulate the hypothesis test for our novel membership inference attack RMIA, as follows:

$$\text{Score}_{\text{MIA}}(x; \theta) = \Pr_{z \sim \pi} (\text{LR}_\theta(x, z) \geq \gamma) \quad (5)$$

We measure the probability that x can γ -dominate a random sample z from the population, for threshold $\gamma \geq 1$. The threshold $\gamma \geq 1$ enables us to adjust how much larger the probability of learning θ with x as a training data should be *relative* to a random alternative point z to pass the test. Figure 7 shows that the test is not very sensitive to small variations of γ .

In summary, the following presents our attack procedure corresponding to the MIA game (we provide a detailed pseudo-code in Appendix B.1).

¹ $\Pr(\theta)$ is canceled from the numerator and denominator.

²See Appendix B.2.1 for alternatives for computing $\Pr(x|\theta)$.

Method	RMIA (this paper)	LiRA [8]	Attack-R [54]	Attack-P [54]	Global [56]
MIA Score	$\Pr_z \left(\frac{\Pr(\theta x)}{\Pr(\theta z)} \geq \gamma \right)$	$\frac{\Pr(\theta x)}{\Pr(\theta \bar{x})}$	$\Pr_{\theta'} \left(\frac{\Pr(x \theta)}{\Pr(x \theta')} \geq 1 \right)$	$\Pr_z \left(\frac{\Pr(x \theta)}{\Pr(z \theta)} \geq 1 \right)$	$\Pr(x \theta)$

Table 1: Computation of $\text{Score}_{\text{MIA}}(x; \theta)$ in different membership inference attacks, where the notation \bar{x} (for LiRA) represents the case where x is not in the training set. The attack is $\text{MIA}(x; \theta) = \mathbb{1}_{\text{Score}_{\text{MIA}}(x; \theta) \geq \beta}$ based on Definition 2.1.

Definition 3.1 (Robust Membership Inference Attack) *Let θ be the target model, and let x be the target data point. Let γ and β be the test parameters. The task is to determine if x was in the training set of θ .*

- i* – Sample many $z \sim \pi$, and compute $\text{Score}_{\text{MIA}}(x; \theta)$ as the fraction of z samples that pass the relative membership inference likelihood ratio test $\text{LR}_{\theta}(x, z) \geq \gamma$. [See equation 5]
- ii* – Return MEMBER if $\text{Score}_{\text{MIA}}(x; \theta) \geq \beta$, and NON-MEMBER otherwise. [See equation 1]

The standard MIA threshold β in equation 1 specifies that there should be a sufficient fraction of the randomly sampled population data to affirm that x is a member. By performing the test over all possible values of $\beta \in [0, 1]$, we compute the ROC power-error trade-off curve.

4 RMIA Interpretation and Improvements over Prior Attacks

Membership inference attacks, framed as hypothesis tests, essentially compute the *relative* likelihood of observing θ given x ’s membership in the training set of θ versus observing θ under x ’s non-membership (null hypothesis). The key to a robust test is accounting for *all information sources* that distinguish these possible worlds. Membership inference attacks use *references* as anchors from the hypothesis worlds, comparing the pair (x, θ) against them. Effectively designing the test involves leveraging all possible informative references, which could be either population data or models trained on them. MIA methods predominantly focus on using reference models. The *way* that such reference models are used matters a lot. As we show in our empirical evaluation, prior state-of-the-art attacks [8, 54] exhibit different behavior depending on the reference models (i.e., in different scenarios, they *dominate each other in opposing ways*). Also, even though they outperform attacks that are based on population data by a large margin, they do not strictly dominate them on all membership inference queries [54]. They, thus, fall short due to overlooking some type of relativity.

Table 1 summarizes the MIA scores of various attacks. Our method offers a fresh perspective on the problem. This approach leverages both population data and reference models, enhancing attack power and robustness against changes in adversary’s background knowledge. Our likelihood ratio test, as defined in equation 5 and equation 3, effectively measures the distinguishability between x and any z based on the shifts in their probabilities when conditioned on θ , through contrasting $\Pr(x|\theta)/\Pr(x)$ versus $\Pr(z|\theta)/\Pr(z)$. The prior work could be seen as partial *uncalibrated* versions of our test. Attack-P [54] and related methods [43, 9, 4] rely primarily on how the likelihood of the target model on x and z change, and neglect or fail at accurately capturing the $\Pr(x)/\Pr(z)$ term of the test. The strength of our test lies in its ability to detect subtle differences in $\Pr(x|\theta)/\Pr(z|\theta)$ and $\Pr(z)/\Pr(x)$ LR, which reflects the noticeable change in LR due to the inclusion of x in the target training set. By repeatedly applying

this RMIA test for numerous z samples from the population, our membership inference attack gains a strong confidence in distinguishing members from non-members.

Stronger prior attacks utilizing reference models, especially as seen in [54] and similar attacks [50], neglect the $\Pr(z|\theta)/\Pr(z)$ component of our test. Calibration by z would tell us if the magnitude of $\Pr(x|\theta)/\Pr(x)$ is significant (compared to non-members), without which the attacks would under-perform throughout the TPR-FPR curve. LiRA [8] falters in the same way, missing the essential calibration of their test with population data.³ But, the unreliability of LiRA is not only because of this. To explain this, let us first introduce an alternative method to compute our LR equation 2.

In the black-box setting, the divergence between the two (numerator and denominator) distributions in a MIA likelihood ratio is a stationary point *when* the model is queried on the differing points [55]. This has been the practice in MIA attacks. So, the best strategy to maximize the likelihood ratio in the black-box setting is to evaluate $f_\theta(x_{\text{features}})$ and $f_\theta(z_{\text{features}})$, where $f_\theta(\cdot)$ is a classification model with parameters θ . Thus, a **direct** way to compute equation 2 is the following:

$$\text{LR}_\theta(x, z) = \frac{\Pr(\theta|x)}{\Pr(\theta|z)} \approx \frac{\Pr(f_\theta(x), f_\theta(z)|x)}{\Pr(f_\theta(x), f_\theta(z)|z)}, \quad (6)$$

where the terms can be computed as in Appendix B.5 and [8]. We provide an empirical comparison between attack performance of our main computation (equation 3 using Bayes rule) and direct computations of the likelihood ratio in Appendix B.5. The results show that our construction of RMIA using the Bayes rule equation 3 is very robust and dominates the direct computation of LR equation 6 when a few reference models are used (Figure 10), and they match when we use a large number of reference models (Figure 9). Thus, our attack strictly dominates LiRA [8] throughout the power-error (TPR-FPR) curve, and the gap increases significantly when we limit the budget for reference models (See Figure 15). The combination of a pairwise LR and its computation using the Bayesian approach results in our robust, high-power, and low-cost attack.

5 Empirical Evaluation

In this section, we present a comprehensive empirical evaluation of RMIA and compare its performance with the prior state-of-the-art attacks. Our goal is to analyze:

1. Performance of attacks under *limited computation resources* for training reference models. This includes limiting the attack to the offline mode where reference models are pre-trained.
2. *Ultimate power of attacks* when unlimited number of reference models could be trained.
3. The strength of the attacks in distinguishing members from non-members when target data points are *out-of-distribution*. This reflects the *resilience and usefulness* of attacks for acting as an oracle for partitioning the entire data space into members and non-members.
4. Impact of *adversary's knowledge* on the performance of attacks (in particular data distribution shift about the population data, and mismatch of network architecture between target and reference models).

³By applying the Bayes rule on the numerator of LiRA LR and considering that the denominator is the same as $\Pr(\theta)$ when the OUT reference models are sampled from the population (and not a small finite set), the LiRA $\text{Score}_{\text{MIA}}(x; \theta)$ is $\Pr(x|\theta)/\Pr(x)$.

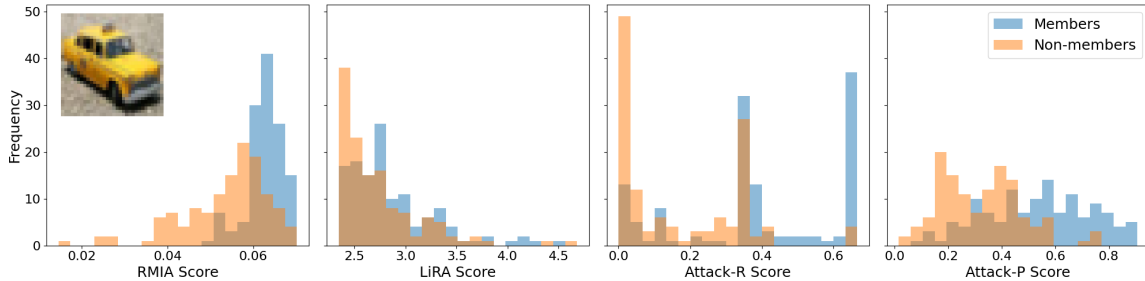


Figure 2: Distribution of $\text{Score}_{\text{MIA}}(x; \theta)$ obtained for a given test sample from CIFAR-10, computed on 127 models where the data is a *member* versus 127 models where the same data is a *non-member*. See more examples in Figure 21.

Setup. We perform our experiments on CIFAR-10, CIFAR-100, CINIC-10 and Purchase-100, which are benchmark datasets commonly used for MIA evaluations. We use the standard metrics, notably the FPR versus TPR curve, and the area under the ROC curve (AUC), for analyzing attacks. The setup of our experiments, including the description of datasets, models, hyper-parameters, and metrics, is explained in details in Appendix A.

Attack Modes (offline vs. online). Reference models are trained on population samples [20, 42, 43, 54, 50]. Adversaries can also train reference models incorporating the target data (MIA query) [8], to design strong tests simulating the leave-one-out scenario [55], despite the impracticality of online training on arbitrary queries. In the context of online attacks, we refer to models trained with the query as IN models, and to those without as OUT models. In the offline mode, all reference models are OUT.

Baseline Attacks. We compare the performance of RMIA with the state-of-the-art attacks [54, 8] which had been shown to outperform their prior methods [50, 43, 44, 40, 32, 56, 21]. The work of [54, 8] remain the strongest attacks since their publication compared with the more recent efficient attacks notably Bertran et al. [4].⁴ In summary, we use Attack-P [54] as an attack that does not use any reference models, Attack-R [54] which uses reference models in an offline mode, and LiRA [8] which is an inference attack in online and offline modes. Our attack RMIA operates in both offline and online modes (see Appendix B.2.2).

5.1 Illustrating Distinguishability Power of MIA Score

Strong inference attacks compute $\text{Score}_{\text{MIA}}(x; \theta)$ in such a way that it accurately reflects the distinguishability between models that are trained on a target data point and the ones that are not. For a better understanding of the distinctions between attacks, Figure 2 illustrates the distribution of MIA scores obtained from various attacks for a given test sample. We compute $\text{Score}_{\text{MIA}}(x; \theta)$ on 254 target models, with the car sample being a member to half of them and a non-member to the other half. The attacks are conducted using 127 OUT reference models in an offline mode. The MIA score produced by RMIA contributes to a more apparent separation between members and non-members (member scores tend to concentrate in the right part of the

⁴See Bertran et al. [4][Table 4] which shows relative weakness of the attack on benchmark datasets such as CIFAR-10, CIFAR-100, and CINIC-10, even when the baseline method [8] uses a few reference models.

# Ref Models	Attack	CIFAR-10			CIFAR-100			CINIC-10		
		AUC	TPR@FPR		AUC	TPR@FPR		AUC	TPR@FPR	
			0.01%	0.0%		0.01%	0.0%		0.01%	0.0%
0	Attack-P	58.19 \pm 0.33	0.01	0.00	75.91 \pm 0.36	0.01	0.00	66.91 \pm 0.30	0.01	0.00
1	Attack-R	63.65 \pm 0.27	0.07	0.02	81.61 \pm 0.17	0.06	0.02	72.04 \pm 0.35	0.07	0.02
	LiRA	53.20 \pm 0.23	0.48	0.25	68.95 \pm 0.28	0.54	0.27	59.93 \pm 0.40	0.32	0.07
	RMIA	68.64 \pm 0.43	1.19	0.51	87.18 \pm 0.14	2.06	0.77	79.00 \pm 0.29	0.86	0.31
2	Attack-R	63.35 \pm 0.30	0.32	0.08	81.52 \pm 0.21	0.31	0.06	72.02 \pm 0.32	0.21	0.07
	LiRA	54.42 \pm 0.34	0.67	0.27	72.21 \pm 0.28	1.52	0.76	62.18 \pm 0.47	0.57	0.26
	LiRA (Online)	63.97 \pm 0.35	0.76	0.43	84.55 \pm 0.16	1.15	0.55	73.17 \pm 0.29	0.53	0.12
	RMIA	70.13 \pm 0.37	1.71	0.91	88.92 \pm 0.20	4.90	1.73	80.56 \pm 0.29	2.14	0.98
4	Attack-R	63.52 \pm 0.29	0.65	0.21	81.78 \pm 0.19	0.63	0.19	72.18 \pm 0.27	0.40	0.14
	LiRA	54.60 \pm 0.25	0.97	0.57	73.57 \pm 0.31	2.26	1.14	63.07 \pm 0.41	1.03	0.45
	LiRA (Online)	67.00 \pm 0.33	1.38	0.51	87.82 \pm 0.20	3.64	2.19	77.06 \pm 0.29	1.34	0.51
	RMIA	71.02 \pm 0.37	2.91	2.13	89.81 \pm 0.17	7.05	3.50	81.46 \pm 0.31	3.20	1.39

Table 2: Performance of attacks where a **few reference models** are used. All attacks, except LiRA, are **low-cost and offline** (do not need new reference models to be trained per query). Results are averaged over 10 random target models.

plot, as opposed to other attacks). In Appendix C.7, we show the variation in MIA scores of all samples in all attacks.

5.2 Inference Attack under Low Computation Budget

Using a Few Reference Models. Figure 1 shows the TPR versus FPR tradoff curves for all attacks when the number of reference models are limited to 1. Obviously, RMIA outperforms both Attack-R and LiRA across all FPR values. Table 2 compares the result of attacks in a low-cost scenario where the adversary has access to only a limited number of reference models. Our focus is on attacks in offline mode, where a fixed number of reference models are pre-trained and used to perform the inference on all queries. We also include LiRA (Online) as a benchmark, despite its high computation cost (half reference models need to be trained on the target data).

Our proposed RMIA demonstrates its strict dominance over the prior work across all datasets. For instance, with only 2 CIFAR-10 reference models, it achieves around 10% higher AUC than both Attack-R and LiRA and still gains at least 110% better TPR at zero FPR. It is important to highlight that, RMIA (in offline mode) also dominates LiRA (Online) . For example, with 4 CIFAR-10 models, it has at least 6% higher AUC and a significant 3x improvement for TPR at zero FPR, compared to LiRA (Online) . In the extreme case of using one single reference model, RMIA shows at least 26% higher AUC and 100% more TPR at low FPRs than LiRA over all datasets. Attack-R outperforms LiRA (Offline) and results in a relatively high AUC, but it does not perform as well at lower FPR regions. Also, Attack-P does not use any reference models, yet it outperforms LiRA in the offline mode.

Using More Reference Models in the Offline Mode. Table 3 compares the performance of offline attacks when using a larger number of OUT models (127 models). The RMIA consistently outperforms other offline attacks across all datasets. RMIA has a much larger power than the Attack-R (which is the strongest offline attack in the prior work). Attack-R may wrongly reject a typical member as a non-member solely because it has a higher probability in reference models. As a result, it yields 5%-10% lower AUC than RMIA across all datasets. RMIA is designed to overcome these limitations by considering both the characteristics of the target sample

Attack	CIFAR-10				CIFAR-100				CINIC-10				Purchase-100			
	AUC	TPR@FPR		AUC	TPR@FPR		AUC	TPR@FPR		AUC	TPR@FPR		AUC	TPR@FPR		AUC
		0.01%	0.0%		0.01%	0.0%		0.01%	0.0%		0.01%	0.0%		0.01%	0.0%	
Attack-R	64.41 \pm 0.41	1.52	0.80	83.37 \pm 0.24	4.80	2.59	73.64 \pm 0.34	2.17	1.12	77.80 \pm 0.41	1.02	0.42				
LiRA	55.18 \pm 0.37	1.37	0.72	75.78 \pm 0.33	2.53	1.13	64.51 \pm 0.51	1.33	0.60	65.82 \pm 0.58	0.31	0.11				
RMIA	71.71 \pm 0.43	4.18	3.14	90.57 \pm 0.15	11.45	6.16	82.33 \pm 0.32	5.07	3.33	83.21 \pm 0.33	2.35	0.69				
LiRA (online)	72.04 \pm 0.47	3.39	2.01	91.48 \pm 0.16	10.85	7.13	82.44 \pm 0.30	4.43	2.92	83.23 \pm 0.37	1.99	0.82				
RMIA (online)	72.25 \pm 0.46	4.31	3.15	91.01 \pm 0.14	11.35	7.78	82.70 \pm 0.35	6.77	4.43	83.90 \pm 0.36	2.56	1.29				

Table 3: Performance of attacks using a large number of reference models, averaged over 10 random target models. The top part (the first three rows) represents offline attacks, using 127 OUT reference models. The second part (the bottom two rows) represents online attacks, using 127 OUT and 127 IN models. Note the larger AUC of RMIA as well as its significant TPR at very small FPR.

within reference models and its relative probability among other population records.

Comparing Table 3 and Table 2 shows that the AUC of RMIA when using a few reference models is almost the same as that of using a large number (127) of models. This shows that the overall power of the attack is not significantly dependent on having many reference models. However, when we increase the number of reference models the attack TPR in low FPR regions increases.

5.3 Ultimate Power of (Online) Inference Attacks

Table 3 presents the performance of all attacks on models trained with different datasets where we have enough resources to train many (254 IN and OUT) reference models. In this setting, RMIA (Online) performs slightly better than LiRA (Online) with respect to AUC. In this case, even minor AUC improvements are particularly significant when closely approaching the true leakage of the training algorithm through hundreds of trained models. However, what is very important to note is that *RMIA (Online) ’s TPR at zero FPR is significantly better than that of LiRA (Online) (by up to 50%)*. It is also important to note that our offline attack achieves performance comparable to online attacks across all datasets, which is quite remarkable, considering the training costs associated with online models. See also Appendix C.1 for the illustration of attacks’ TPR versus FPT tradeoff curves, using various number of models trained on different datasets.

We can further improve attacks by querying the target model with multiple augmentations of input query, obtained via simple mirror and shift operations on image data. See Appendix B.4 for the details. RMIA can leverage this technique to a significantly greater extent, and can achieve *a 4x improvement in TPR at zero FPR and about 4.6% higher AUC* compared to LiRA .

5.4 Dependency on Availability of Reference Models

Inference attacks must be robust to changes in their assumptions about the prior knowledge of adversary, for example population data available to train reference models. Low-cost MIA methods should also be less dependent on availability of a large number of reference models.

Figure 3 presents the number of reference models needed to achieve an overall performance for attacks (computed using their AUC). Note that online attacks need at least 2 reference models (1 IN, 1 OUT). While increasing the number of reference models improves the performance of all

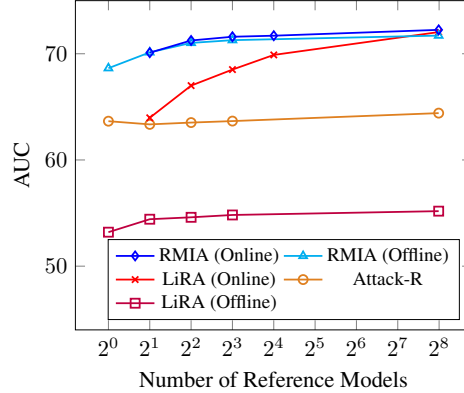


Figure 3: The number of reference models versus the overall performance of the attacks (RMIA vs. Attack-R and LiRA on CIFAR-10). In online attacks, half of reference models need to be trained per each MIA query.

attacks, RMIA consistently outperforms others, particularly with a limited number of reference models. Remarkably, the RMIA (Offline) is stronger than LiRA (Online) attacks unless when use hundreds of reference models.

RMIA does gain from increasing the number of reference models, but even with a small number of models, it is very close to its maximal overall performance. However, LiRA (Online) displays a great sensitivity to the changes in number of reference models (with a huge AUC gap of about 8% in CIFAR-10 models when comparing 2 models versus 254 models), underscoring the necessity of a large number of models for this attack to function effectively. Appendix C.1 presents additional AUC results with other datasets.

5.5 Reliability of MIA Tests for OOD Data

We challenge membership inference attacks by testing them with non-member out-of-distribution (OOD) data. A strong MIA should be able to rule out *all non-members* regardless of whether they are from the same distribution as its training data or not. This is of a great importance also in scenarios where we might use MIA oracles in applications such as data extraction attacks [7]. In such cases, it is essential for the attack to remain accurate (high TPR for all FPR) in the on out-of-distribution (OOD) test samples. To examine this, we train our models with CIFAR-10 and use samples from a different dataset (CINIC-10) to generate OOD non-member test queries. We focus on offline attacks, as it is practically infeasible to train IN models for each and every individual OOD test sample, especially when dealing with a large volume of queries.

Figure 4 illustrates the ROC curves. RMIA has a substantial performance advantage (at least 21% higher AUC) over other attacks, with RMIA not performing much better than random guessing. Conducting our hypothesis test by assessing the pair-wise LR between the target sample x and several *in-distribution* z samples enables us to capture significant differences between $\frac{\Pr(x|\theta)}{\Pr(x)}$ and $\frac{\Pr(z|\theta)}{\Pr(z)}$ in equation 3 to effectively distinguish OOD queries from members. We also present the result of using pure noise as test queries in Appendix C.2.

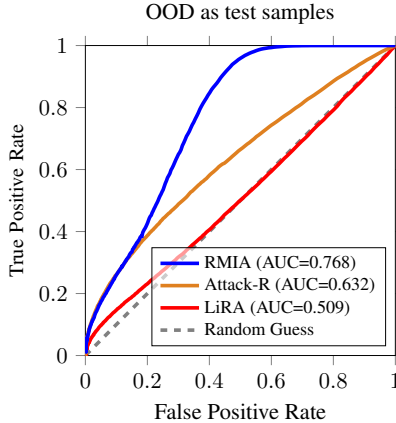


Figure 4: ROC of three offline attacks using models trained on CIFAR-10, while non-member test queries are OOD samples from CINIC-10. We use 127 reference models.

5.6 Robustness to Model and Data Distribution Shift

When assessing membership inference attacks, it is crucial to examine how the attack’s performance is influenced when the adversary lacks precise knowledge about the distribution of training data and also the structure of the target model. Therefore, we compare the result of attacks when the reference models are trained on different datasets than the target models. More specifically, the target models are trained on CIFAR-10, while the reference models are trained on CINIC-10. The performance of all attacks is affected when there is a data distribution shift between the training set of the target model and the reference models. However, compared with other attacks, RMIA always obtains a higher AUC (e.g. by up to 25% in comparison with LiRA, using 2 reference models) and a better TPR at low FPRs. We present the detailed result of this experiment in Appendix C.3.

We also study the impact of network architecture change between the target model and the reference models. While the optimal performance of all attacks is noted when both the target and reference models share a similar architecture, the superiority of our attack becomes more pronounced in the presence of architecture shifts (we observe up to 3% increase in the AUC gap between our attack and others). See Appendix C.4 for the details of the empirical results.

5.7 Analyzing RMIA Parameters

Number of z samples. Our attack evaluates the likelihood ratio of the target model on a target data x versus other population samples z . We train our reference models on population samples. The same samples could be used in our test to compute the pair-wise LR values. Computing the LR versus the population samples enables us to compute reliable test statistics for our attack. Table 4 shows how the result of RMIA changes, as we use different number of reference samples. The AUC increases when we increase the number of z samples, but it is noteworthy that using 2500 population samples, equivalent to 10% of the size of the models’ training set, yields results comparable to those obtained with a 10 fold larger population set. Moreover, the TPR at low FPRs is still high even when we consider just 250 reference samples. In the default setting, we use all non-members of a target model as the set of z samples.

# population samples z	AUC	TPR@FPR	
		0.01%	0.0%
25 samples	58.71 ± 0.26	1.32	1.15
250 samples	64.88 ± 0.24	2.23	1.65
1250 samples	67.57 ± 0.30	2.22	1.73
2500 samples	68.25 ± 0.27	2.26	1.72
6250 samples	68.78 ± 0.31	2.28	1.75
12500 samples	69.03 ± 0.33	2.28	1.77
25000 samples	69.15 ± 0.35	2.26	1.80

Table 4: Performance of RMIA (Online) using different number of random z samples. The number of reference models, trained on CIFAR-10, is 254 (127 IN, 127 OUT).

Sensitivity to Pair-Wise LR Test Threshold γ . The result of our experiments, presented in Appendix B.3, shows that our attack’s performance is consistent against changes in the value of γ . Both AUC and FPR-TPR curve remain relatively stable with small changes to γ (except for a considerably high value of γ). In fact, by adjusting the value of the threshold β , we achieve roughly the same result across different γ values. In Appendix B.3, we study the selection of γ parameter and its relation to β .

5.8 Applying RMIA to Other ML Algorithms

To assess how attacks perform against alternative training algorithms, we investigate the impact of using the DP-SGD and also the Gradient Boosting Decision Tree (GBDT) for training models. As depicted in Appendix C.5, RMIA surpasses other attacks in terms of the obtained AUC when training models with DP-SGD, although the performance of all attacks tends to converge to random guessing in more stringent settings. In the case of training with GBDT, the TPR obtained by our attack consistently outperforms all other attacks, particularly by an order of magnitude at zero FPR, as demonstrated in Appendix C.6.

6 Related Work

Neural networks, particularly when trained with privacy-sensitive datasets, have been proven to be susceptible to leaking information about their training data. A variety of attacks have been designed to gauge the degree of leakage and the subsequent privacy risk associated with training data. For instance, *data extraction attacks* attempt to recreate individual samples used in training the model [7], whereas *model inversion attacks* focus on extracting aggregate information about specific sub-classes instead of individual samples [16]. In contrast, *property inference attacks* derive non-trivial properties of samples in a target model’s training dataset [17]. This paper, however, is concerned with *membership inference attacks (MIAs)*, which predict whether a particular sample was used in the training process of the model. MIAs, due to their simplicity, are commonly utilized as auditing tools to quantify data leakage in trained models.

MIAs first found their use in the realm of genome data to identify the presence of an individual’s genome in a mixed batch of genomes [20]. [2] went on to formalize the risk analysis for identifying an individual’s genome from aggregate statistics on independent attributes, with this analysis later extended to include data with dependent attributes [35].

Algorithms featuring differential privacy (DP) are designed to limit the success rate of privacy attacks when distinguishing between two neighboring datasets [38]. Some researches, such as

[47], provide upper limits on the average success of MIAs on general targets. Other studies evaluate the effectiveness of MIAs on machine learning models trained with DP algorithms [39].

[43] introduced membership inference attacks for machine learning algorithms. The work demonstrated the efficacy of membership inference attacks against machine learning models in a setting where the adversary has query access to the target model. This approach was based on the training of reference models, also known as shadow models, with a dataset drawn from the same distribution as the training data. Subsequent works extended the idea of shadow models to different scenarios, including white-box [24, 37, 40] and black-box settings [44, 19, 11], label-only access [12, 26], and diverse datasets [41]. However, such methods often require the training of a substantial number of models upon receiving an input query, making them unfeasible due to processing and storage costs, high response times, and the sheer amount of data required to train such a number of models. MIA has been also applied in other machine learning scenarios, such as federated learning [37, 34, 48] and multi-exit networks [27].

Various mechanisms have been proposed to defend against MIAs, although many defense strategies have proven less effective than initially reported [44]. Since the over-fitting issue is an important factor affecting membership leakage, several regularization techniques have been used to defend against membership inference attacks, such as L2 regularization, dropout and label smoothing [43, 41, 31]. Some recent works try to mitigate membership inference attacks by reducing the target model’s generalization gap [25, 10] or self-distilling the training dataset [46]. [1] proposed DP-SGD method which adds differential privacy [14] to the stochastic gradient descent algorithm. Subsequently, some works concentrated on reducing the privacy cost of DP-SGD through adaptive clipping or adaptive learning rate [57, 53]. In addition, there are defense mechanisms, such as AdvReg [36] and MemGuard [22], that have been designed to hide the distinctions between the output posteriors of members and non-members.

Recent research has emphasized evaluating attacks by calculating their true positive rate (TPR) at a significantly low false positive rate (FPR) [8, 54, 30, 32, 50]. For example, [8] found that many previous attacks perform poorly under this evaluation paradigm. They then created an effective attack based on a likelihood ratio test between the distribution of models that use the target sample for training (IN models) and models that do not use it (OUT models). Despite the effectiveness of their attack, especially at low FPRs, it necessitates the training of many reference models to achieve high performance. [50] constructed a membership inference attack incorporating sample hardness and using each sample’s hardness threshold to calibrate the loss from the target model. [54] proposed a template for defining various MIA games and a comprehensive hypothesis testing framework to devise potent attacks that utilize reference models to significantly improve the TPR for any given FPR. [30] presented an attack which utilizes trajectory-based signals generated during the training of distilled models to effectively enhance the differentiation between members and non-members. The recent paper [52] has improved the performance of likelihood test-driven attacks by estimating a variant of the target sample through minimally perturbing the original sample, which minimizes the fitting loss of IN and OUT shadow models. Lately, [23] have introduced a novel privacy notion called f -MIP, which allows for bounding the trade-off between the power and error of attacks using a function f . This is especially applicable when models are trained using gradient updates. The authors demonstrated the use of DP-SGD to achieve this f -MIP bound. Additionally, they proposed a cost-effective attack for auditing the privacy leakage of ML models, with the assumption that the adversary has white-box access to gradients of the target model.

A number of related work tune the threshold β in MIA based on the data point. Chang

and Shokri [9] improve the attack by determining the threshold for a data point, based on its attributes (e.g., data points corresponding to the same gender are used as the reference population to determine the threshold corresponding to a given FPR.) When it is not very easy to identify the reference population, Bertran et al. [4] train an attack model for each FPR threshold to determine the threshold associated with the reference population.

Some recent studies have focused on low-cost auditing of differentially private deep learning algorithms. This is a different setting in terms of the problem statement, yet it is aligned with the spirit of our work that aims at reducing the auditing cost. Steinke et al. [45] outline an efficient method for auditing differentially private machine learning algorithms. Their approach achieves this with a single training run, leveraging parallelism in the addition or removal of multiple training examples independently.

In alignment with MIA research [42, 35, 54, 8], we highlight the power (TPR) of MIAs at extremely low errors (FPR). We propose a different test that allows us to devise a new attack that reaps the benefits of various potent attacks. The attack proposed in this paper demonstrates superior overall performance and a higher TPR at zero FPR than the attacks introduced by [8, 54], especially when only a limited number of reference models are trained. Additionally, it maintains high performance in an offline setting where none of the reference models are trained with the target sample. This characteristic renders our attack suitable for practical scenarios where resources, time, and data are limited.

7 Conclusions

We argue that MIA tests, as privacy auditing tools, must be stress tested with low computation budget, few available reference models, and changes to data and models. A strong test is the one that outperform others in these scenarios.

Acknowledgements

The authors would like to thank Vincent Bindschaedler and Jiayuan Ye for their valuable feedback and constructive technical discussions related to this work.

References

- [1] Martín Abadi, Andy Chu, Ian Goodfellow, H. Brendan McMahan, Ilya Mironov, Kunal Talwar, and Li Zhang. Deep learning with differential privacy. In *Proceedings of the 23rd ACM SIGSAC Conference on Computer and Communications Security (CCS’16)*, page 308–318, 2016.
- [2] Michael Backes, Pascal Berrang, Mathias Humbert, and Praveen Manoharan. Membership privacy in microrna-based studies. In *Proceedings of the 23rd ACM SIGSAC Conference on Computer and Communications Security (CCS’16)*, page 319–330, 2016.
- [3] Kunal Banerjee, Vishak C. Prasad, Rishi Raj Gupta, Karthik Vyas, Anushree H, and Biswajit Mishra. Exploring alternatives to softmax function. In *Proceedings of the 2nd International Conference on Deep Learning Theory and Applications (DeLTA’21)*, page 81–86, 2021.

- [4] Martin Bertran, Shuai Tang, Michael Kearns, Jamie Morgenstern, Aaron Roth, and Zhiwei Steven Wu. Scalable membership inference attacks via quantile regression. In *Proceedings of the 37th Conference on Neural Information Processing Systems (NeurIPS'23)*, 2023.
- [5] Charles Blundell, Julien Cornebise, Koray Kavukcuoglu, and Daan Wierstra. Weight uncertainty in neural network. In *International conference on machine learning*, pages 1613–1622. PMLR, 2015.
- [6] Nicholas Carlini, Chang Liu, Úlfar Erlingsson, Jernej Kos, and Dawn Song. The secret sharer: Evaluating and testing unintended memorization in neural networks. In *28th USENIX Security Symposium (USENIX Security'19)*, page 267–284, 2019.
- [7] Nicholas Carlini, Florian Tramer, Eric Wallace, Matthew Jagielski, Ariel Herbert-Voss, Katherine Lee, Adam Roberts, Tom Brown, Dawn Song, Ulfar Erlingsson, and et al. Extracting training data from large language models. In *30th USENIX Security Symposium (USENIX Security'21)*, 2021.
- [8] Nicholas Carlini, Steve Chien, Milad Nasr, Shuang Song, Andreas Terzis, and Florian Tramer. Membership inference attacks from first principles. In *IEEE Symposium on Security and Privacy (S&P'22)*, page 1897–1914, 2022.
- [9] Hongyan Chang and Reza Shokri. On the privacy risks of algorithmic fairness. In *2021 IEEE European Symposium on Security and Privacy (EuroS&P)*, pages 292–303. IEEE, 2021.
- [10] Dingfan Chen, Ning Yu, and Mario Fritz. Relaxloss: Defending membership inference attacks without losing utility. In *Proceedings of the 10th International Conference on Learning Representations (ICLR'22)*, 2022.
- [11] Min Chen, Zhikun Zhang, Tianhao Wang, Michael Backes, Mathias Humbert, and Yang Zhang. When machine unlearning jeopardizes privacy. In *Proceedings of the 28th ACM SIGSAC Conference on Computer and Communications Security (CCS '21)*, page 896–911, 2021.
- [12] Christopher A. Choquette-Choo, Florian Tramer, Nicholas Carlini, and Nicolas Papernot. Label-only membership inference attacks. In *Proceedings of the 38th International Conference on Machine Learning (ICML'21)*, page 1964–1974, 2021.
- [13] Alexandre De Brebisson and Pascal Vincent. An exploration of softmax alternatives belonging to the spherical loss family. In *Proceedings of the 4th International Conference on Learning Representations (ICLR'16)*, 2016.
- [14] Cynthia Dwork. Differential privacy. In *Proceedings of 33rd International Colloquium in Automata, Languages and Programming (ICALP'06)*, page 1–12, 2006.
- [15] Cynthia Dwork, Adam Smith, Thomas Steinke, Jonathan Ullman, and Salil Vadhan. Robust traceability from trace amounts. In *2015 IEEE 56th Annual Symposium on Foundations of Computer Science*, pages 650–669. IEEE, 2015.

- [16] Matt Fredrikson, Somesh Jha, and Thomas Ristenpart. Model inversion attacks that exploit confidence information and basic countermeasures. In *Proceedings of the 22nd ACM SIGSAC Conference on Computer and Communications Security (CCS'15)*, page 1322–1333, 2015.
- [17] Karan Ganju, Qi Wang, Wei Yang, Carl A Gunter, and Nikita Borisov. Property inference attacks on fully connected neural networks using permutation invariant representations. In *Proceedings of the 25th ACM SIGSAC Conference on Computer and Communications Security (CCS'18)*, page 619–633, 2018.
- [18] Kaiming He, Xiangyu Zhang, Shaoqing Ren, , and Jian Sun. Deep residual learning for image recognition. In *Proceedings of the IEEE Conference on Computer Vision and Pattern Recognition (CVPR'16)*, 2016.
- [19] Sorami Hisamoto, Matt Post, and Kevin Duh. Membership inference attacks on sequence-to-sequence models: Is my data in your machine translation system? *Transactions of the Association for Computational Linguistics*, 8:49–63, 2020.
- [20] Nils Homer, Szabolcs Szelinger, Margot Redman, David Duggan, Waibhav Tembe, Jill Muehling, John V Pearson, Dietrich A Stephan, Stanley F Nelson, and David W Craig. Resolving individuals contributing trace amounts of dna to highly complex mixtures using high-density snp genotyping microarrays. *PLoS Genetics*, 4(8), 2008.
- [21] Bargav Jayaraman, Lingxiao Wang, Katherine Knipmeyer, Quanquan Gu, and David Evans. Revisiting membership inference under realistic assumptions. *arXiv preprint arXiv:2005.10881*, 2020.
- [22] Jinyuan Jia, Ahmed Salem, Michael Backes, Yang Zhang, and Neil Zhenqiang Gong. Mem-guard: Defending against black-box membership inference attacks via adversarial examples. In *Proceedings of the 26th ACM SIGSAC Conference on Computer and Communications Security (CCS'19)*, page 259–274, 2019.
- [23] Tobias Leemann, Martin Pawelczyk, and Gjergji Kasneci. Gaussian membership inference privacy. In *Proceedings of the 37th Conference on Neural Information Processing Systems (NeurIPS'23)*, 2023.
- [24] Klas Leino and Matt Fredrikson. Stolen memories: Leveraging model memorization for calibrated white-box membership inference. In *29th USENIX Security Symposium (USENIX Security'20)*, page 1605–1622, 2020.
- [25] Jiacheng Li, Ninghui Li, and Bruno Ribeiro. Membership inference attacks and defenses in classification models. In *Proceedings of the 11th ACM Conference on Data and Application Security and Privacy (CODASPY'21)*, page 5–16, 2021.
- [26] Zheng Li and Yang Zhang. Membership leakage in label-only exposures. In *Proceedings of the 28th ACM SIGSAC Conference on Computer and Communications Security (CCS'21)*, page 880–895, 2021.
- [27] Zheng Li, Yiyong Liu, Xinlei He, Ning Yu, Michael Backes, and Yang Zhang. Auditing membership leakages of multi-exit networks. In *Proceedings of the 29th ACM SIGSAC Conference on Computer and Communications Security (CCS'22)*, page 1917–1931, 2022.

- [28] Xuezhi Liang, Xiaobo Wang, Zhen Lei, Shengcai Liao, and Li Stan Z. Soft-margin softmax for deep classification. In *Proceedings of the 24th International Conference on Neural Information Processing (ICONIP'17)*, page 413–421, 2017.
- [29] Weiyang Liu, Yandong Wen, Zhiding Yu, and Meng Yang. Large-margin softmax loss for convolutional neural networks. In *Proceedings of the 33rd International Conference on Machine Learning (ICML'16)*, 2016.
- [30] Yiyong Liu, Zhengyu Zhao, Michael Backes, and Zhang Yang. Membership inference attacks by exploiting loss trajectory. In *Proceedings of the 29th ACM SIGSAC Conference on Computer and Communications Security (CCS'22)*, page 2085–2098, 2022.
- [31] Yugeng Liu, Rui Wen, Xinlei He, Ahmed Salem, Zhikun Zhang, Michael Backes, Emiliano De Cristofaro, Mario Fritz, and Yang Zhang. ML-doctor: Holistic risk assessment of inference attacks against machine learning models. In *31st USENIX Security Symposium (USENIX Security'22)*, page 4525–4542, 2022.
- [32] Yunhui Long, Lei Wang, Diyue Bu, Vincent Bindschaedler, Xiaofeng Wang, Haixu Tang, Carl A Gunter, and Kai Chen. A pragmatic approach to membership inferences on machine learning models. In *IEEE European Symposium on Security and Privacy (EuroS&P'20)*, page 521–534, 2020.
- [33] David JC MacKay. *Information theory, inference and learning algorithms*. Cambridge university press, 2003.
- [34] Luca Melis, Congzheng Song, Emiliano De Cristofaro, and Vitaly Shmatikov. Exploiting unintended feature leakage in collaborative learning. In *IEEE Symposium on Security and Privacy (S&P'19)*, page 691–706, 2019.
- [35] Sasi Kumar Murakonda, Reza Shokri, and George Theodorakopoulos. Quantifying the privacy risks of learning high-dimensional graphical models. In *Proceedings of the International Conference on Artificial Intelligence and Statistics*, page 2287–2295, 2021.
- [36] Milad Nasr, Reza Shokri, and Amir Houmansadr. Machine learning with membership privacy using adversarial regularization. In *Proceedings of the 25th ACM SIGSAC Conference on Computer and Communications Security (CCS'18)*, page 634–646, 2018.
- [37] Milad Nasr, Reza Shokri, and Amir Houmansadr. Comprehensive privacy analysis of deep learning: Passive and active white-box inference attacks against centralized and federated learning. In *IEEE Symposium on Security and Privacy (S&P'19)*, page 1022–1036, 2019.
- [38] Milad Nasr, Shuang Song, Abhradeep Thakurta, Nicolas Papernot, and Nicholas Carlini. Adversary instantiation: Lower bounds for differentially private machine learning. In *IEEE Symposium on Security and Privacy (S&P'21)*, page 866–882, 2021.
- [39] Md Atiqur Rahman, Tanzila Rahman, Robert Laganieri, Noman Mohammed, and Yang Wang. Membership inference attack against differentially private deep learning model. *Transactions on Data Privacy*, 11(1):61–79, 2018.
- [40] Alexandre Sablayrolles, Matthijs Douze, Cordelia Schmid, Yann Ollivier, and Hervé Jégou. White-box vs black-box: Bayes optimal strategies for membership inference. In *Proceedings*

- of the 36th International Conference on Machine Learning (ICML'19), page 5558–5567, 2019.
- [41] Ahmed Salem, Yang Zhang, Mathias Humbert, Mario Fritz, and Michael Backes. Ml-leaks: Model and data independent membership inference attacks and defenses on machine learning models. In *Network and Distributed Systems Security Symposium (NDSS'19)*, 2019.
 - [42] Sriram Sankararaman, Guillaume Obozinski, Michael I Jordan, and Eran Halperin. Genomic privacy and limits of individual detection in a pool. *Nature genetics*, 41(9):965–967, 2009.
 - [43] Reza Shokri, Marco Stronati, Congzheng Song, and Vitaly Shmatikov. Membership inference attacks against machine learning models. In *IEEE Symposium on Security and Privacy (S&P'17)*, page 3–18, 2017.
 - [44] Liwei Song and Prateek Mittal. Systematic evaluation of privacy risks of machine learning models. In *30th USENIX Security Symposium (USENIX Security'21)*, pages 2615–2632, 2021.
 - [45] Thomas Steinke, Milad Nasr, and Matthew Jagielski. Privacy auditing with one (1) training run. *Proceedings of the 37th Conference on Neural Information Processing Systems (NeurIPS'23)*, 2023.
 - [46] Xinyu Tang, Saeed Mahloujifar, Liwei Song, Virat Shejwalkar, Milad Nasr, Amir Houmansadr, and Prateek Mittal. Mitigating membership inference attacks by self-distillation through a novel ensemble architecture. In *31st USENIX Security Symposium (USENIX Security'22)*, pages 1433–1450, 2022.
 - [47] Anvith Thudi, Ilia Shumailov, Franziska Boenisch, and Nicolas Papernot. Bounding membership inference. In *arXiv preprint*, page arXiv:2202.12232, 2022.
 - [48] Stacey Truex, Ling Liu, Mehmet Emre Gursoy, Lei Yu, and Wenqi Wei. Demystifying membership inference attacks in machine learning as a service. *IEEE Transactions on Services Computing*, 14(6):2073–2089, 2019.
 - [49] Peter M Visscher and William G Hill. The limits of individual identification from sample allele frequencies: theory and statistical analysis. *PLoS genetics*, 5(10):e1000628, 2009.
 - [50] Lauren Watson, Chuan Guo, Graham Cormode, and Alex Sablayrolles. On the importance of difficulty calibration in membership inference attacks. In *Proceedings of the 10th International Conference on Learning Representations (ICLR'22)*, 2022.
 - [51] Lauren Watson, Chuan Guo, Graham Cormode, and Alexandre Sablayrolles. On the importance of difficulty calibration in membership inference attacks. In *Proceedings of International Conference on Learning Representations (ICLR'22)*, 2022.
 - [52] Yuxin Wen, Arpit Bansal, Hamid Kazemi, Eitan Borgnia, Micah Goldblum, Jonas Geiping, and Tom Goldstein. Canary in a coalmine: Better membership inference with ensembled adversarial queries. In *Proceedings of the 11th International Conference on Learning Representations (ICLR'23)*, 2023.

- [53] Zhiying Xu, Shuyu Shi, Alex X. Liu, Jun Zhao, and Lin Chen. An adaptive and fast convergent approach to differentially private deep learning. In *Proceedings of 39th IEEE International Conference on Computer Communications (Infocom'20)*, page 1867–1876, 2020.
- [54] Jiayuan Ye, Aadyaa Maddi, Sasi Kumar Murakonda, Vincent Bindschaedler, and Reza Shokri. Enhanced membership inference attacks against machine learning models. In *Proceedings of the 29th ACM SIGSAC Conference on Computer and Communications Security (CCS'22)*, page 3093–3106, 2022.
- [55] Jiayuan Ye, Anastasia Borovykh, Soufiane Hayou, and Reza Shokri. Leave-one-out distinguishability in machine learning. *12th International Conference on Learning Representations (ICLR'24)*, 2024.
- [56] Samuel Yeom, Irene Giacomelli, Matt Fredrikson, and Somesh Jha. Privacy risk in machine learning: Analyzing the connection to overfitting. In *2018 IEEE 31st Computer Security Foundations Symposium (CSF'18)*, pages 268–282. IEEE, 2018.
- [57] Lei Yu, Ling Liu, Calton Pu, Mehmet Emre Gursoy, and Stacey Truex. Differentially private model publishing for deep learning. In *IEEE Symposium on Security and Privacy (S&P'19)*, page 332–349, 2019.
- [58] Chiyuan Zhang, Daphne Ippolito, Katherine Lee, Matthew Jagielski, Florian Tramèr, and Nicholas Carlini. Counterfactual memorization in neural language models. *arXiv preprint arXiv:2112.12938*, 2021.

Contents

1	Introduction	1
2	Performing Membership Inference Attacks	3
3	Designing RMIA	3
4	RMIA Interpretation and Improvements over Prior Attacks	5
5	Empirical Evaluation	6
5.1	Illustrating Distinguishability Power of MIA Score	7
5.2	Inference Attack under Low Computation Budget	8
5.3	Ultimate Power of (Online) Inference Attacks	9
5.4	Dependency on Availability of Reference Models	9
5.5	Reliability of MIA Tests for OOD Data	10
5.6	Robustness to Model and Data Distribution Shift	11
5.7	Analyzing RMIA Parameters	11
5.8	Applying RMIA to Other ML Algorithms	12
6	Related Work	12
7	Conclusions	14
A	Experimental Setup	21
B	Details of RMIA and its Evaluation	21
B.1	Pseudo-code of RMIA	21
B.2	Likelihood Ratio Computation in equation 3	23
B.2.1	Computing $\Pr(x \theta)$	23
B.2.2	Computing $\Pr(x)$	23
B.3	Analyzing γ and β Parameters and their Relation	26
B.4	Boosting RMIA with Augmented Queries	27
B.5	Direct Computation of Likelihood Ratio in equation 2	27
C	Supplementary Empirical Results	32
C.1	Performance of Attack Obtained on Different Datasets	32
C.2	Robustness of Attacks against Noise and OOD	38
C.3	Data Distribution Shift	38
C.4	Variations in Neural Network Architectures	39
C.5	Attacking DP-SGD	40
C.6	Performance of Attacks on Models Trained with other ML Algorithms	41
C.7	MIA Score Comparison between Attacks	41

A Experimental Setup

To conduct attacks, we must first train models. We adopt the same training setup as in [8], wherein, for a given dataset, we train our models on randomly selected training sets, with each set containing half of the dataset. Moreover, each sample of the dataset is included in exactly half of the reference models’ training set. We pick our target models from the set of trained models at random. It is worth noting that in this setting, the training set of a target model can overlap by 50% with each reference model.

Datasets. We report the attack results on models trained on four different datasets, traditionally used for membership inference attack evaluations. For CIFAR-10 [18] (a traditional image classification dataset), we train a Wide ResNets (with depth 28 and width 2) to 92% test accuracy (for 100 epochs) on half of the dataset (25000 samples, chosen at random). For CIFAR-100 and CINIC-10 (as other image datasets), we follow the same process as for CIFAR-10 and train a wide ResNet on half of the dataset to get 67% and 77% test accuracy, respectively, surpassing the accuracy of models used in prior studies. We set the batch size to 256. We also include the result of attacks on Purchase-100 dataset (a tabular dataset of shopping records) [43], where models are 4-layer MLP with layer units=[512, 256, 128, 64], trained on 25k samples for 50 epochs to obtain 83% test accuracy. We train our models using standard techniques to reduce over-fitting, including train-time augmentations, weight decay and early stopping. Exactly like [8], there are a number of simple augmentations for each training sample in image models, computed by horizontally flipping and/or shifting the image by a few pixels. As a result, the train-test accuracy gap of our models is small (e.g. below 7% for CIFAR-10 models).

Evaluation Metrics. We measure the performance of each attack using two underlying metrics: its true positive rate (TPR), and its false positive rate (FPR), over all member and non-member records of random target models. Then, we use the ROC curve to reflect the trade-off between the TPR and FPR of an attack, as we sweep over all possible values of threshold β to build different FPR tolerance. The AUC (area under the ROC curve) score gives us the average success across all target samples and measures the overall strength of an attack. Inspired from previous discussions in [8], we also consider TPR at very low FPRs. More precisely, we focus on TPR at 0% FPR, a metric that has seen limited usage in the literature. When attacking a target model, all samples in the population data are used as input queries. Hence, for each target model, half of queries are members and the other half are non-members.

B Details of RMIA and its Evaluation

B.1 Pseudo-code of RMIA

Membership inference attacks require training reference (or shadow) models in order to distinguish members from non-members of a given target model. We train k reference models on a set of samples randomly drawn from the population data. Concerning the training of models, we have two versions of RMIA. The RMIA (Online) (similar to [8]) trains reference models separately for each target data (MIA test query). Specifically, upon receiving a MIA test query x , we train k IN models that include x in their training set. However, such a training is costly and impractical in many real-world scenarios due to the significant resource and time requirements. On the other hand, the offline version uses only k pre-trained reference models on randomly

Algorithm 1 MIA Score Computation with RMIA. The input to this algorithm is k reference models Θ , the target model θ , target (test) sample x , parameter γ , and a scaling factor a as described in Appendix B.2.2. We assume the reference models Θ are pre-trained on random samples from a population dataset available to adversary; each sample from the population dataset is included in training of $k/2$ reference models. The algorithm also takes an *online* flag which indicates whether we intend to run MIA in the online mode.

```

1: Randomly choose a subset  $Z$  from the population dataset
2:  $C \leftarrow 0$ 
3: if online then
4:    $\Theta_{in} \leftarrow \emptyset$ 
5:   for  $k$  Times do
6:      $D_i \leftarrow$  randomly sample a dataset from population data  $\pi$ 
7:      $\theta_x \leftarrow \mathcal{T}(D_i \cup x)$ 
8:      $\Theta_{in} \leftarrow \Theta_{in} \cup \{\theta_x\}$ 
9:      $\Pr(x) \leftarrow \frac{1}{2k} (\sum_{\theta' \in \Theta} \Pr(x|\theta') + \sum_{\theta' \in \Theta_{in}} \Pr(x|\theta'))$       (See equation 9)
10:  else
11:     $\Pr(x)_{OUT} \leftarrow \frac{1}{k} \sum_{\theta' \in \Theta} \Pr(x|\theta')$ 
12:     $\Pr(x) \leftarrow \frac{1}{2} ((a+1) \cdot \Pr(x)_{OUT} + (1-a))$       (See Appendix B.2.2)
13:   $Ratio_x \leftarrow \frac{\Pr(x|\theta)}{\Pr(x)}$ 
14:  for each sample  $z$  in  $Z$  do
15:     $\Pr(z) \leftarrow \frac{1}{k} \sum_{\theta' \in \Theta} \Pr(z|\theta')$ 
16:    if offline then
17:       $\Pr(z) \leftarrow \frac{1}{2} ((a+1) \Pr(z) + (1-a))$ 
18:     $Ratio_z \leftarrow \frac{\Pr(z|\theta)}{\Pr(z)}$ 
19:    if  $(Ratio_x / Ratio_z) > \gamma$  then
20:       $C \leftarrow C + 1$ 
21:  $Score_{MIA}(x; \theta) \leftarrow C/|Z|$       (See equation 5)

```

sampled datasets, avoiding any training on test queries (as it exclusively uses OUT models). The two versions differ in the way they compute the normalizing term $\Pr(x)$ in equation 3. The online algorithm computes the terms by averaging prediction probabilities over all IN and OUT models in an unbiased manner (equation 9), while the offline algorithm computes the terms solely with OUT models based on equation 10. In the offline mode, we approximate what $\Pr(x)$ would have been if we had access to IN models (see Appendix B.2.2 for more explanations).

Algorithm 1 outlines the pseudo-code for RMIA. The input to this algorithm includes the target model θ , the target sample x , the threshold γ , and the set of reference models denoted by Θ , which are trained prior to computing the MIA score of x . Additionally, it takes an *online* flag indicating if we run the algorithm in online mode. If it we are in offline mode, a scaling factor a is also obtained as described in Appendix B.2.2. The output of the algorithm is $Score_{MIA}(x; \theta)$, which is then used according to equation 1 to infer the membership of x . As described in Algorithm 1, we first select our reference population samples (i.e., the set Z) from the population dataset. If we are operating in the online mode, we train k IN models using target data x and a randomly selected dataset from the population data (line 5-8). Depending on the attack mode, we query the reference models to obtain the average prediction probabilities over reference models as $\Pr(x)$ (line 9 and line 11). In the case of offline RMIA, line 12 approximates

$\Pr(x)$ using equation 10. Then, we calculate the ratio of prediction probabilities between the target model and the reference models for sample x as $Ratio_x$ (line 13). The same routine is applied to obtain the ratio for each reference sample $z \in Z$ (line 15-18).

According to equation 3, the division of the computed ratio for sample x by the obtained ratio for sample z determines $LR_\theta(x, z)$ to assess if z is γ -dominated by x (line 19). The fraction of γ -dominated reference samples establishes the MIA score of the target sample x in RMIA (line 21).

B.2 Likelihood Ratio Computation in equation 3

B.2.1 Computing $\Pr(x|\theta)$

Let θ be a classification (neural network) model that maps each input data x to a probability distribution across d classes. Assume data point x is in class y . Let $c(x) = \langle c_1, \dots, c_d \rangle$ be the output vector (logits) of the neural network for input x , before applying the final normalization. We denote the normalized prediction probability of class y for the input x as $f_\theta(x)_y$. For the Softmax function, the probability is given by

$$f_\theta(x)_y = \frac{e^{\frac{c_y}{T}}}{\sum_{i=1}^d e^{\frac{c_i}{T}}},$$

where T is a temperature constant. We can use this to estimate $\Pr(x|\theta)$. However, there are many alternatives to Softmax probability proposed in the literature to improve the accuracy of estimating $\Pr(x|\theta)$, using the Taylor expansion of the exponential function, and using heuristics to refine the relation between the probabilities across different classes [13, 29, 28, 3]. In this paper, we use the following to compute $\Pr(x|\theta)$ for image datasets:

$$f_\theta(x)_y = \frac{apx(c_y - m)}{apx(c_y - m) + \sum_{i \neq y} apx(c_i)}, \quad (7)$$

where $apx(a) = \sum_{i=0}^n \frac{a^i}{i!}$ is the n th order Taylor approximation of e^a , and m is a hyper-parameter that controls the separation between probability of different classes.

In Table 5, we compare the result of RMIA obtained with four different prediction likelihood functions, i.e. Softmax, Taylor-Softmax [13], Soft-Margin Softmax (SM-Softmax) [28], and the combination of last two functions (SM-Taylor-Softmax) [3], formulated in equation 7. Based on our empirical results, we set the soft-margin m and the order n in Taylor-based functions to 0.6 and 4, respectively. The temperature (T) is set to 2 for CIFAR-10 models. While the performance of all functions is closely comparable, SM-Taylor-Softmax stands out by achieving a slightly higher AUC and a rather better TPR at low FPRs. In Figure 5, we present the performance sensitivity of our attack in terms of AUC concerning three hyper-parameters in this function: order n , soft-margin m , and temperature T . The AUC of RMIA appears to be robust to variations in n , m and T . For $n \geq 3$, the results are consistent, but employing lower orders leads to a poor Taylor-based approximation for Softmax, as reported in other works [3].

B.2.2 Computing $\Pr(x)$

Recall that $\Pr(x)$ is the normalizing constant for the Bayes rule in computing our LR. See equation 4. We compute it as the empirical average of $\Pr(x|\theta')$ on reference models θ' trained

Likelihood Function	AUC	TPR@FPR	
		0.01%	0.0%
Softmax	68.96 ± 0.31	2.25	1.69
SM-Softmax	69.02 ± 0.34	2.27	1.67
Taylor-Softmax	68.57 ± 0.29	2.06	1.43
SM-Taylor-Softmax	69.15 ± 0.35	2.26	1.80

Table 5: Performance of RMIA obtained with various prediction likelihood functions. The number of reference models, trained with CIFAR-10, is 254. The soft-margin m and the order n in Taylor-based functions are 0.6 and 4, respectively.

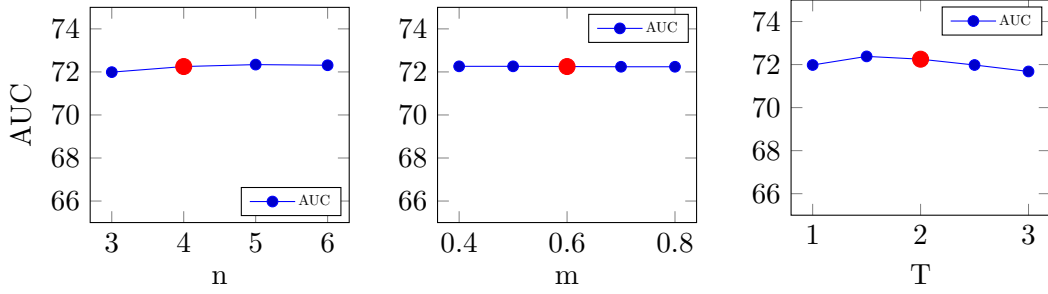


Figure 5: AUC of our attack (RMIA) obtained by using different values of n (order in Taylor function), m (soft-margin) and T (temperature) in SM-Taylor-Softmax function. When modifying one parameter, we hold the values of the other two parameters constant at their optimal values. Here, we use 254 reference models trained on CIFAR-10. Results are averaged over 10 target models. The red points indicate the default values used in our experiments.

on random datasets D drawn from the population distribution π . This is then used in pairwise likelihood ratio equation 3.

In order to compute $\Pr(x)$, we need to train reference models θ' . Note that the reference models must be sampled in an unbiased way with respect to whether x is part of their training data. This is because the summation in equation 4 is over all θ' , which can be partitioned to the set of models trained on x (IN models), and the set of models that are not trained on x (OUT models). Let \bar{x} denote that a training set does not include x . Let θ'_x denote an IN model trained on dataset D_x ($x \in D_x$) and $\theta'_{\bar{x}}$ be an OUT model trained on dataset $D_{\bar{x}}$ ($x \notin D_{\bar{x}}$). Then, from equation 4, we have:

$$\begin{aligned}
\Pr(x) &= \sum_{\theta', D} \Pr(x|\theta') \Pr(\theta'|D) \Pr(D) \\
&= \sum_{\theta'_x, D_x} \Pr(x|\theta'_x) \Pr(\theta'_x|D_x) \Pr(D_x) + \sum_{\theta'_{\bar{x}}, D_{\bar{x}}} \Pr(x|\theta'_{\bar{x}}) \Pr(\theta'_{\bar{x}}|D_{\bar{x}}) \Pr(D_{\bar{x}})
\end{aligned} \tag{8}$$

The two sums on the right-hand side of the above equation can be computed empirically using sampling methods. Instead of integrating over all possible datasets and models, we sample datasets D_x and $D_{\bar{x}}$ and models θ'_x and $\theta'_{\bar{x}}$, and compute the empirical average of $\Pr(x|\theta'_x)$ and $\Pr(x|\theta'_{\bar{x}})$ given the sampled models. We sample $D_{\bar{x}}$ from the probability distribution $\Pr(D_{\bar{x}})$, which is the underlying data distribution π . For sampling D_x , we sample a dataset from π and add x to the dataset. We sample θ'_x and $\theta'_{\bar{x}}$ by training models on D_x and $D_{\bar{x}}$, respectively.

In the online setting for MIA, we can empirically estimate $\Pr(x)$ by computing the average

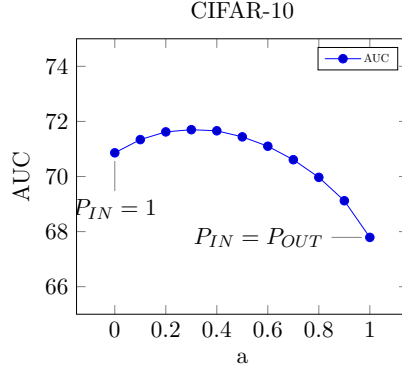


Figure 6: AUC of offline RMIA obtained by using different values of a in the linear approximation function. Here, we use 127 reference models (OUT) trained on CIFAR-10.

$\Pr(x|\theta')$ over 50% IN models and 50% OUT models (using $2k$ models), i.e.:

$$\Pr(x) \approx \underbrace{\frac{1}{2} \left(\frac{1}{k} \sum_{\theta'_x} \Pr(x|\theta'_x) \right)}_{\Pr(x)_{IN}} + \underbrace{\frac{1}{2} \left(\frac{1}{k} \sum_{\theta'_x} \Pr(x|\theta'_x) \right)}_{\Pr(x)_{OUT}} \quad (9)$$

However, in the offline setting, we do not have access to IN models. Thus, we need to exclusively use $\Pr(x|\theta'_x)$. We now introduce a simple heuristic to obtain a less biased estimate of $\Pr(x)$ without having access to IN models, through an offline pre-computation to approximate the shift of probability between IN and OUT models. Essentially, we approximate the sensitivity of models (the gap between probability of member and non-member points in reference models). See Figure 1 in [58] for such computation.

We use our existing reference models to compute the rate at which $\Pr(x)$ for any sample x changes between reference models that include x versus the others. We approximate the gap with a linear function, so we obtain $\Pr(x)_{IN} = a \cdot \Pr(x)_{OUT} + b$, and finally can obtain $\Pr(x) = (\Pr(x)_{IN} + \Pr(x)_{OUT})/2$. Given that both $\Pr(x)_{IN}$ and $\Pr(x)_{OUT}$ fall within the range of 0 to 1, it follows that $a + b = 1$. Consequently, we can simplify the linear function as $\Pr(x)_{IN} = a \cdot (\Pr(x)_{OUT} - 1) + 1$ which results in:

$$\Pr(x) \approx \frac{1}{2} ((a + 1) \Pr(x)_{OUT} + (1 - a)) \quad (10)$$

In Figure 6, we present the AUC obtained by our offline RMIA on CIFAR-10 models, varying the value of a from 0 to 1. As a approaches 1, there is a degradation in AUC (by up to 5.5%), because we heavily rely on $\Pr(x)_{OUT}$ to approximate $\Pr(x)_{IN}$. Lower values of a result in an enhancement of $\Pr(x)_{OUT}$ to approximate $\Pr(x)_{IN}$, leading to improved performance. The AUC appears to be more robust against lower values of a , particularly those below 0.5. Notably, even with $a = 0$, where $\Pr(x) = (\Pr(x)_{OUT} + 1)/2$, a considerable improvement in results is observed. In this case, we are alleviating the influence of very low $\Pr(x)_{OUT}$ for atypical/hard samples.

To determine the best value of a for each dataset, we use the following procedure. It is executed only once, independent of test queries, without the need to train any new models. We choose two existing models and then, select one as the temporary target model and subject it to attacks from the other model using varying values of a . Finally, we select the one that

yields the highest AUC as the optimal a . Based on the result of our experiments, this optimal a remains roughly consistent across random selections of reference models. In our experiments, we empirically derived the following values for our datasets: $a = 0.3$ for CIFAR-10 and CINIC-10, $a = 0.6$ for CIFAR-100, and $a = 0.2$ for Purchase-100 models.

B.3 Analyzing γ and β Parameters and their Relation

We here investigate the impact of selecting γ on the efficacy of our attack. In Figure 7, we illustrate the sensitivity of our attack, measured in terms of AUC and FPR@TPR, to changes in the value of γ . We do not show the result for $\gamma < 1$, because it implies that a target sample x is allowed to have a lower chance of being member than reference samples to pass our pairwise likelihood ratio test, causing lots of non-members to be wrongly inferred as member. As it can be seen from the figure, our attack’s performance is consistent against changes in the value of γ ; both AUC and FPR@TPR remain relatively stable with increasing γ (except for a considerably high value of γ). As γ increases, the need arises to decrease the value of β in the hypothesis test equation (equation 1) to strike a balance between the power and error of the attack. By appropriately adjusting the value of β , we achieve a roughly same result across different γ values. In extreme cases where a very high γ is employed, the detection of γ -dominated reference samples between a limited set of z records becomes exceedingly challenging. We consistently note the same trend in results across all our datasets and with varying numbers of reference models. Throughout our experiments, we set γ to 2, as it yields a slightly higher TPR@FPR.

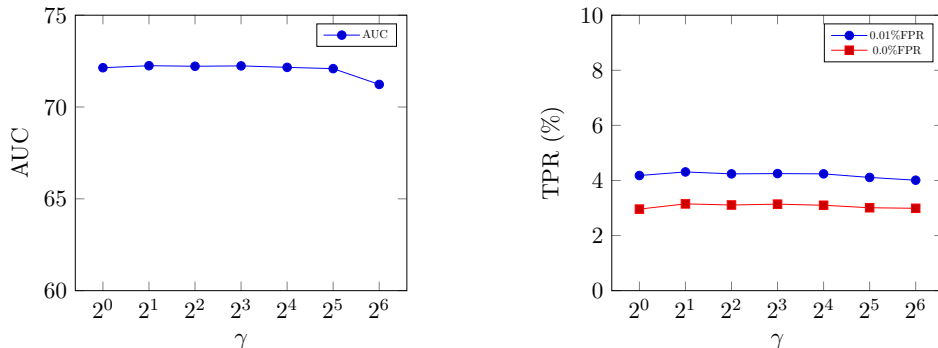


Figure 7: The performance sensitivity of our attack (RMIA) with respect to γ parameter. Here, we use 254 reference models trained on CIFAR-10. The left plot shows the AUC obtained when using different γ values, while the right plot demonstrates the TPR at 0.01% and 0% FPR values versus γ (corresponding to blue and red lines, respectively).

As we discussed in Section 3, β is a common threshold among all attacks, and will be used to generate the ROC curve. In our method (as opposed to e.g., [8]), the exact value of β is interpretable. Specifically, when γ equals 1, the value of β shows a strong correlation with the value of $1 - \text{FPR}$. To show this, Figure 8 illustrates the impact of selecting β from the range $[0, 1]$ on the TPR and FPR of RMIA. We use two distinct γ values: $\gamma = 1$ (shown in the left plot) and $\gamma = 2$ (depicted in the right plot). Both TPR and FPR approach zero, as we increase β to 1 (under both γ values) and the reason is that it is unlikely that a target sample can dominate most of reference records. However, FPR decreases more rapidly than TPR in two plots, especially with $\gamma = 2$, which allows us to always have a higher power gain than error. When $\gamma = 1$, FPR decreases in a calibrated manner, proportional to $1 - \beta$.

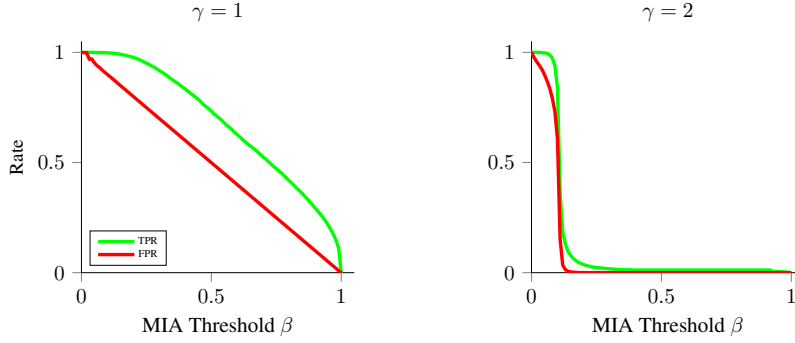


Figure 8: TPR and FPR achieved by RMIA for different values of β . The left and right plots correspond to $\gamma = 1$ and $\gamma = 2$, respectively. The number of reference models, trained with CIFAR-10, is 254.

B.4 Boosting RMIA with Augmented Queries

We can further enhance the effectiveness of RMIA by augmenting the input query x with multiple data samples that are similar to x [8, 12]. These data samples can be simple transformations of x (for example, using shift or rotation in case of image data). To consolidate the results in our multi-query setting, we use majority voting on our hypothesis test in equation 2: x is considered to dominate z if more than half of all generated transformations of x dominate z .

In [8], the authors discussed how to extend LiRA to support multiple queries. We here compare the performance of online and offline attacks when we increase the number of augmented queries from 1 to 50. Note that Attack-P and Attack-R have no result for multiple queries, as they do not originally support query augmentations. In this experiment, we use 254 reference models (for offline attacks, we only use 127 OUT models).

We first compare the offline attacks, shown in the Offline column of Table 6. With no augmented queries, RMIA presents a clear advantage over Attack-R (with 6.7% higher AUC and 116% more TPR at zero FPR) and the performance gap between two attacks widens with using more queries. As we increase queries, RMIA gets a better result (for example, a 4x improvement in TPR at zero FPR and also about 4.6% higher AUC as queries go from 1 to 50), while LiRA cannot benefit from the advantage of more queries to improve its AUC. Note that we use the same technique to generate augmentations, as proposed in [8].

In the Online column of Table 6, we show the result of LiRA and RMIA when all 254 IN and OUT reference models are available to the adversary. Compared to LiRA, RMIA always has a slightly higher AUC and at least 48% better TPR at zero FPR. Note that in this case, even minor AUC improvements are particularly significant when closely approaching the true leakage of the training algorithm through hundreds of models. Both LiRA and RMIA work better with increasing augmented queries, e.g. around 2x improvement in TPR@FPR when going from 1 query to 50 queries. Unless explicitly stated otherwise, the experimental results in this paper are obtained using 18 augmented queries for both LiRA and RMIA.

B.5 Direct Computation of Likelihood Ratio in equation 2

In Section 3, we introduced two separate approaches for computing the fundamental likelihood ratio in equation 2: I) a Bayesian method, as shown by equation 3, and II) a direct method, expressed in equation 6. While our empirical results are primarily derived using the Bayesian

# Queries	Attack	Online			Offline		
		AUC	TPR@FPR		AUC	TPR@FPR	
			0.01%	0.0%		0.01%	0.0%
1	Attack-R	-	-	-	64.41 ± 0.41	1.52	0.80
	Attack-P	-	-	-	58.19 ± 0.33	0.01	0.00
	LiRA	68.92 ± 0.42	1.78	0.92	56.12 ± 0.41	0.46	0.28
	RMIA	69.15 ± 0.35	2.26	1.80	68.74 ± 0.34	2.42	1.73
2	LiRA	71.28 ± 0.46	2.83	1.73	55.77 ± 0.46	1.16	0.59
	RMIA	71.46 ± 0.43	3.69	2.55	71.06 ± 0.39	3.64	2.46
18	LiRA	72.04 ± 0.47	3.39	2.01	55.18 ± 0.37	1.37	0.72
	RMIA	72.25 ± 0.46	4.31	3.15	71.71 ± 0.43	4.18	3.14
50	LiRA	72.26 ± 0.47	3.54	2.19	55.00 ± 0.36	1.52	0.75
	RMIA	72.51 ± 0.46	4.47	3.25	71.95 ± 0.44	4.39	3.22

Table 6: Performance of attacks when we use different number of augmented queries for LiRA [8] and RMIA. We evaluate attacks in two different settings, shown in Online and Offline columns. In the online setting, we use 254 models where half of them are IN models and half are OUT (for each sample). The offline setting uses only 127 OUT models. Both Attack-P and Attack-R [54] do not originally support multiple augmented queries. The Attack-P does not work with reference models, thus we consider it offline. Models are trained with CIFAR-10. Results are averaged over 10 random target models.

method, we anticipate that the outcomes of these two approaches will converge closely when a sufficient number of reference models is employed, although their performance may vary with a limited number of models. In this section, we attempt to assess these two methods and possibly invalidate our initial anticipation.

The direct approach involves employing Gaussian modeling over logits. Our attack is then simplified to the estimation of the mean and variance for the logits of samples x and z in two distinct distributions of reference models; One distribution comprises models trained with x in their training set but not z (denoted by $\theta'_{x,\bar{z}}$), while the other comprises models trained with z in their training set but not x (denoted by $\theta'_{\bar{x},z}$). Let $\mu_{x,\bar{z}}(x)$ and $\sigma_{x,\bar{z}}(x)$ be the mean and variance of $f_{\theta'}(x)$ in the distribution of $\theta'_{x,\bar{z}}$ models, respectively (a similar notation can be defined for $\theta'_{\bar{x},z}$ models). We can approximate the likelihood ratio in equation 6 as follows:

$$\begin{aligned}
\text{LR}_{\theta}(x, z) &\approx \frac{\Pr(f_{\theta}(x), f_{\theta}(z)|x)}{\Pr(f_{\theta}(x), f_{\theta}(z)|z)} \\
&\approx \frac{\Pr(f_{\theta}(x)|\mathcal{N}(\mu_{x,\bar{z}}(x), \sigma_{x,\bar{z}}^2(x)))}{\Pr(f_{\theta}(x)|\mathcal{N}(\mu_{\bar{x},z}(x), \sigma_{\bar{x},z}^2(x)))} \times \frac{\Pr(f_{\theta}(z)|\mathcal{N}(\mu_{x,\bar{z}}(z), \sigma_{x,\bar{z}}^2(z)))}{\Pr(f_{\theta}(z)|\mathcal{N}(\mu_{\bar{x},z}(z), \sigma_{\bar{x},z}^2(z)))} \quad (11)
\end{aligned}$$

where $f_{\theta}(x)$ represents the output (logits) of the target model θ on sample x . Although the direct method may appear to be more straightforward and accurate, it comes with a significantly higher computational cost, since we must train online reference models, i.e. $\theta'_{x,\bar{z}}$, to compute the probabilities in the above relation.

We now demonstrate the performance of our RMIA when the likelihood ratio is computed using equation 3 (hereafter, called RMIA-Bayes), in comparison to using the aforementioned likelihood ratio in equation 11 (referred to as RMIA-direct). Figure 9 compares the ROCs achieved by the two methods when 64 reference models are employed to estimate the probabilities. We show the results obtained from models trained with different datasets (we use no augmented queries). In this case, RMIA-direct slightly outperforms in terms of both AUC and

TPR at low FPRs, yet RMIA-Bayes closely matches its pace, even at low FPR values. On the other hand, Figure 10 presents the scenario where 4 reference models are used. When utilizing fewer models, RMIA-Bayes exhibits a better performance across all datasets (e.g., 6.6% higher AUC in CIFAR-10). It appears that RMIA-direct struggles to accurately estimate the parameters of Gaussian models with only four models available. Given the substantial processing cost of RMIA-direct, associated with training online models relative to sample pairs, RMIA-Bayes emerges as a more reasonable choice due to its ability to operate with a reduced number of models trained in an offline context.

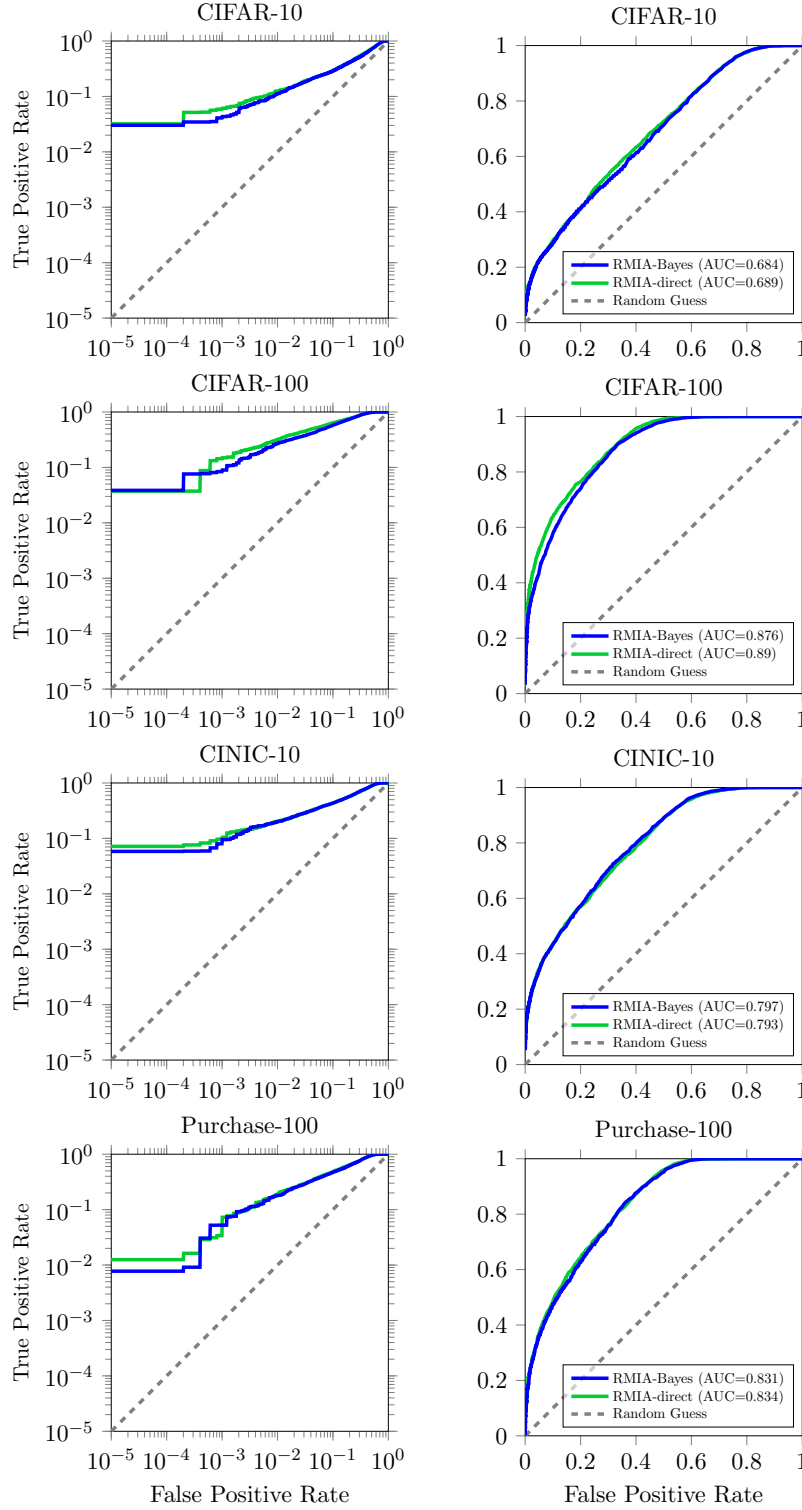


Figure 9: ROC of RMIA when two different methods, i.e. RMIA-direct (as formulated in equation 11) and RMIA-Bayes (based on equation 3), are used to approximate the likelihood ratio. ROCs are shown in both log and normal scales. Here, we use **64 reference models**.

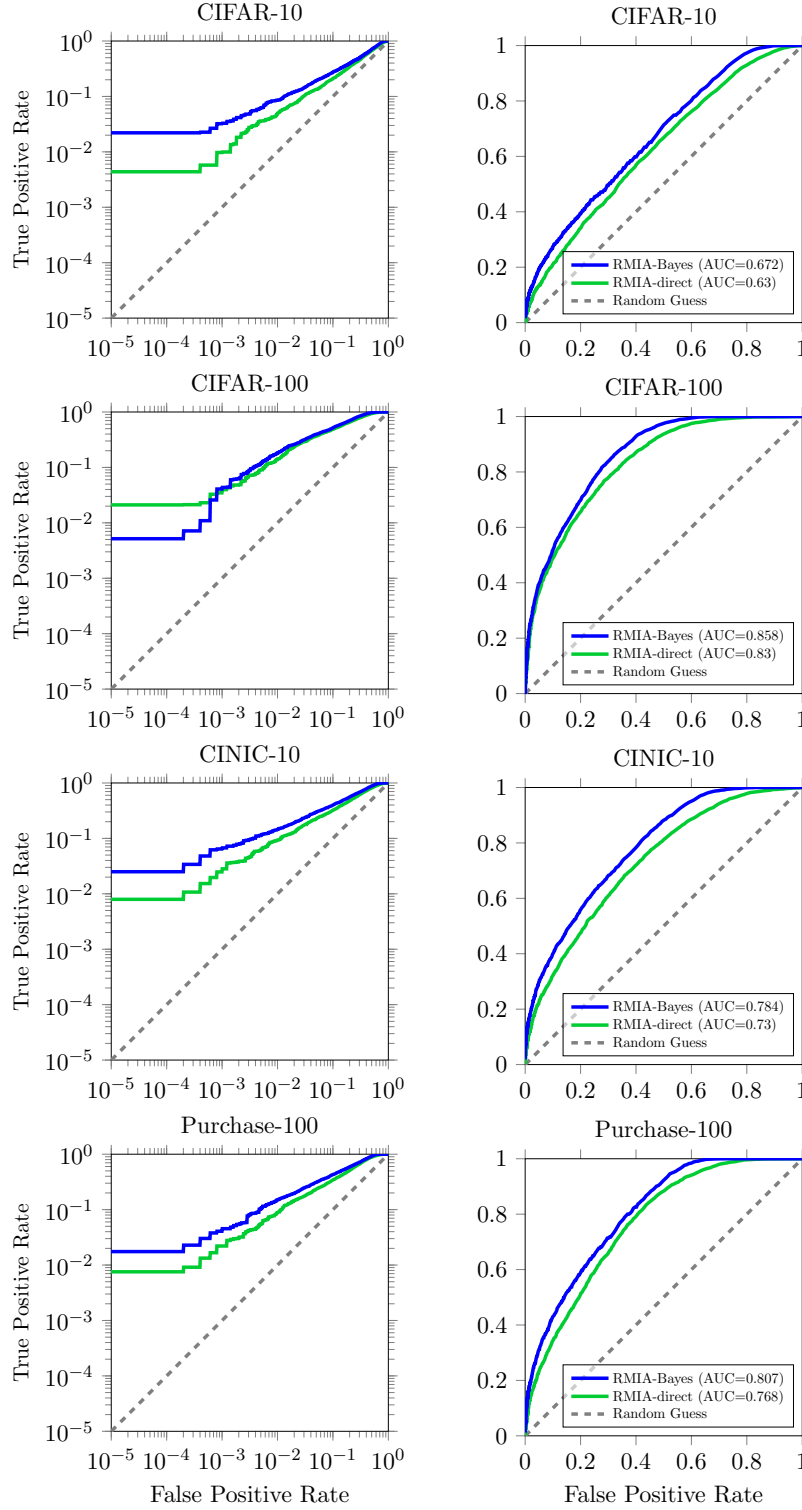


Figure 10: ROC of RMIA when two different methods, i.e. RMIA-direct (as formulated in equation 11) and RMIA-Bayes (based on equation 3), are used to approximate the likelihood ratio. ROCs are shown in both log and normal scales. Here, we use **4 reference models**.

C Supplementary Empirical Results

C.1 Performance of Attack Obtained on Different Datasets

We here compare the ROC of attacks using reference models trained on four different datasets, i.e. CIFAR-10, CIFAR-100, CINIC-10 and Purchase-100. We evaluate attacks when different number of reference models is used. To facilitate a more comprehensive comparison of the overall performance between various attacks, we provide a depiction of the ROC curves in both log and normal scales. In Figure 11, we show the ROC of attacks obtained with using 1 reference model. Since we only have 1 (OUT) model, the result of offline attacks is reported here. RMIA works remarkably better than other three attacks across all datasets. Although LiRA has a rather comparable TPR at low FPR for CIFAR-10 and Purchase-100 models, but it yields a much lower AUC (e.g. 22% lower AUC in CIFAR-10), when compared with RMIA. In other two datasets, RMIA results in around 3 times better TPR at zero FPR, than its closest rival.

Figure 12 displays the ROC of attacks resulted from employing 2 reference model (1 IN, 1 OUT). Again, RMIA works much better than other three attacks (in terms of both AUC and TPR@FPR) across all datasets. For example, it has a 10% higher AUC in CIFAR-10 models and at least 3 times better TPR at zero FPR in CIFAR-100 and CINIC-10, than other attacks. Figure 13 presents the ROC of offline attacks when using 127 OUT models. RMIA works much better than other three attacks across all datasets. For example, it leads to at least 20% higher AUC than LiRA. Figure 14 illustrates the ROC of attacks obtained when using all 254 models (127 IN, 127 OUT models). With the help of training hundreds of IN and OUT models, LiRA can work close to our attack in terms of AUC, but the TPR at zero FPR of RMIA is considerably higher, e.g. by at least 50% in CIFAR-10, CINIC-10 and Purchase-100 models, as compared with LiRA.

For a better comparison between attack performances concerning the number of reference models, Figure 15 presents the AUC results for both offline and online attacks across varying reference model counts (ranging from 1 to 254). The left plots in this figure showcase the outcomes of offline attacks, while the right plots highlight the performance of online attacks. A consistent trend emerges, revealing that an increase in the number of reference models yields an improvement in AUC across all attacks. Notably, in both offline and online scenarios and across all datasets, RMIA consistently outperforms other attacks, particularly when employing a limited number of models. Intriguingly, the results from our offline RMIA, using a small number of reference models (e.g., 4), nearly align with the best outcomes achieved by online algorithms working with hundreds of models.

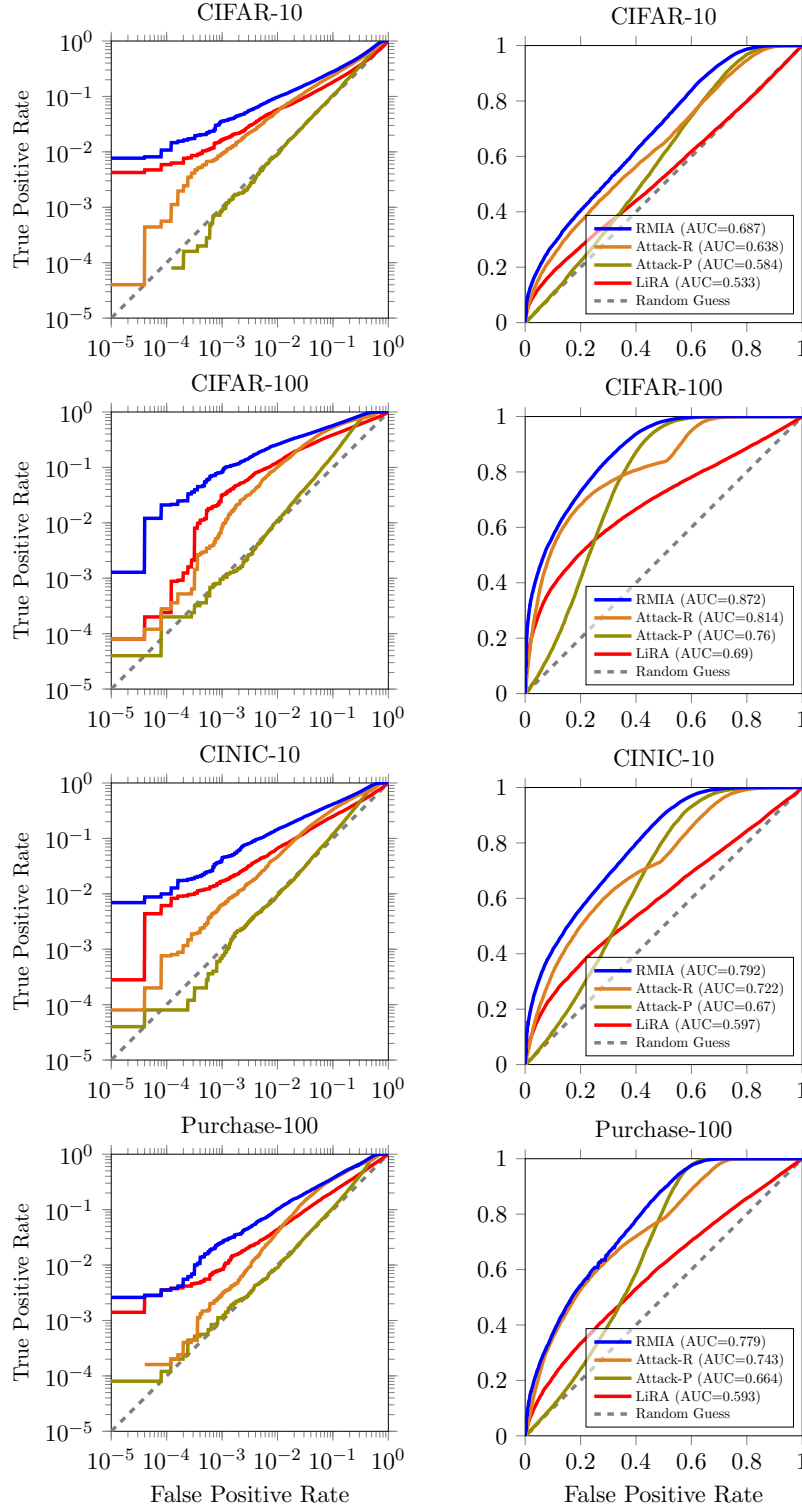


Figure 11: ROC of attacks using models trained on different datasets (ROC's are shown in both log and normal scales). The result is obtained on one random target model. We here use **1 reference model** (OUT).

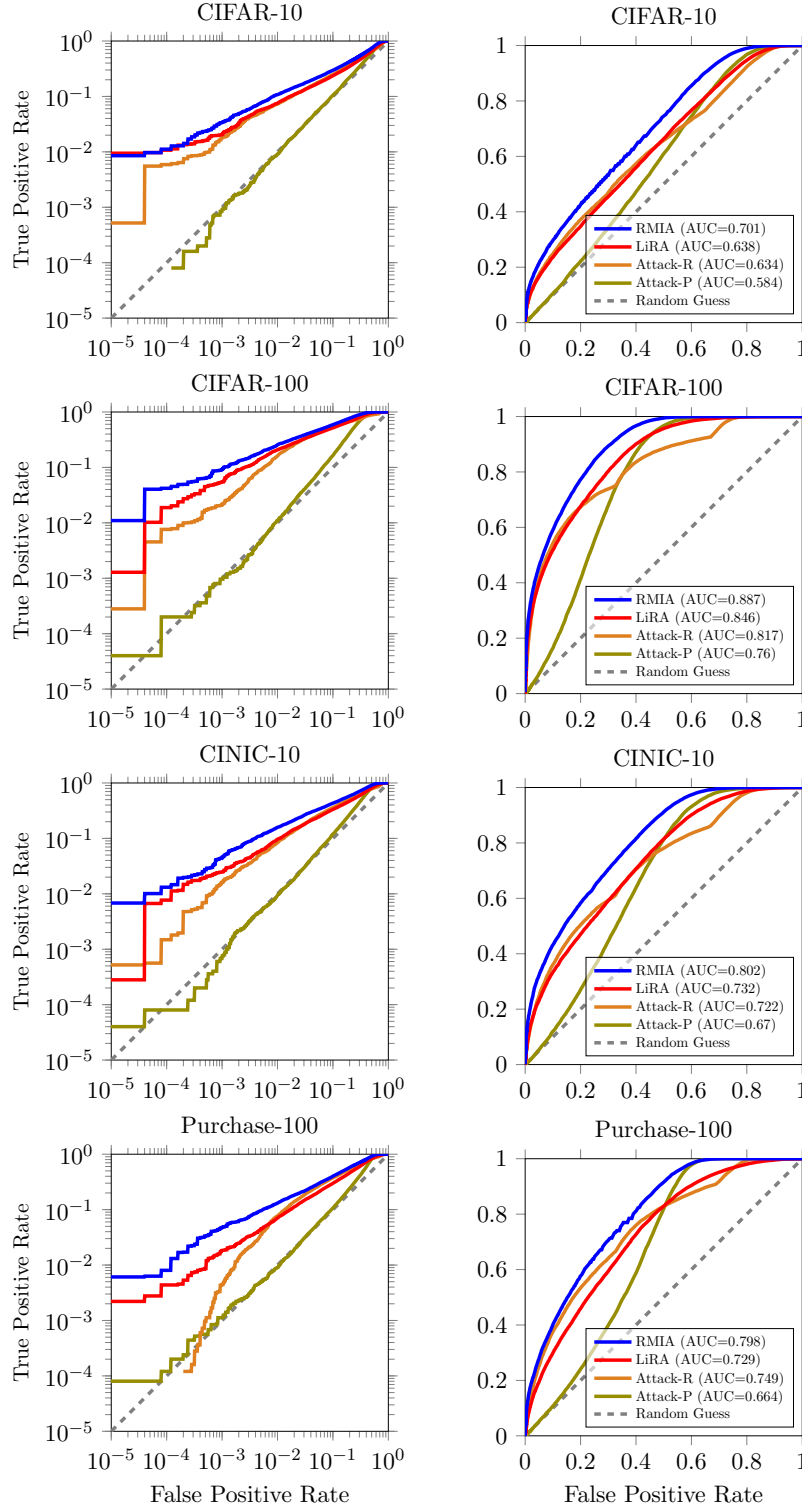


Figure 12: ROC of attacks using models trained on different datasets (ROC are shown in both log and normal scales). The result is obtained on one random target model. We here use **2 reference models** (1 IN, 1 OUT).

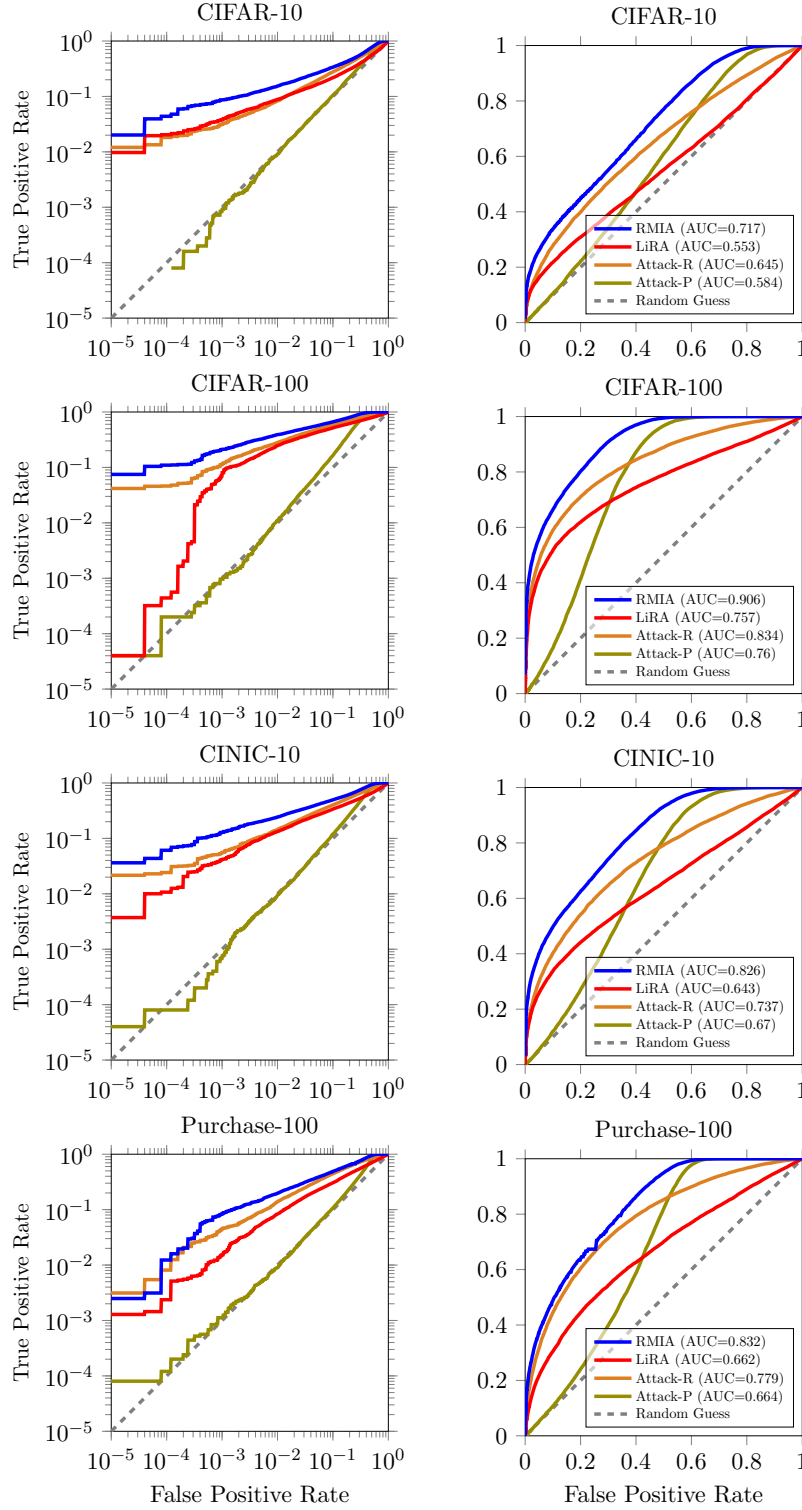


Figure 13: ROC of offline attacks using models trained on different datasets (ROC's are shown in both log and normal scales). The result is obtained on one random target model. We use **127 reference models (OUT)**.

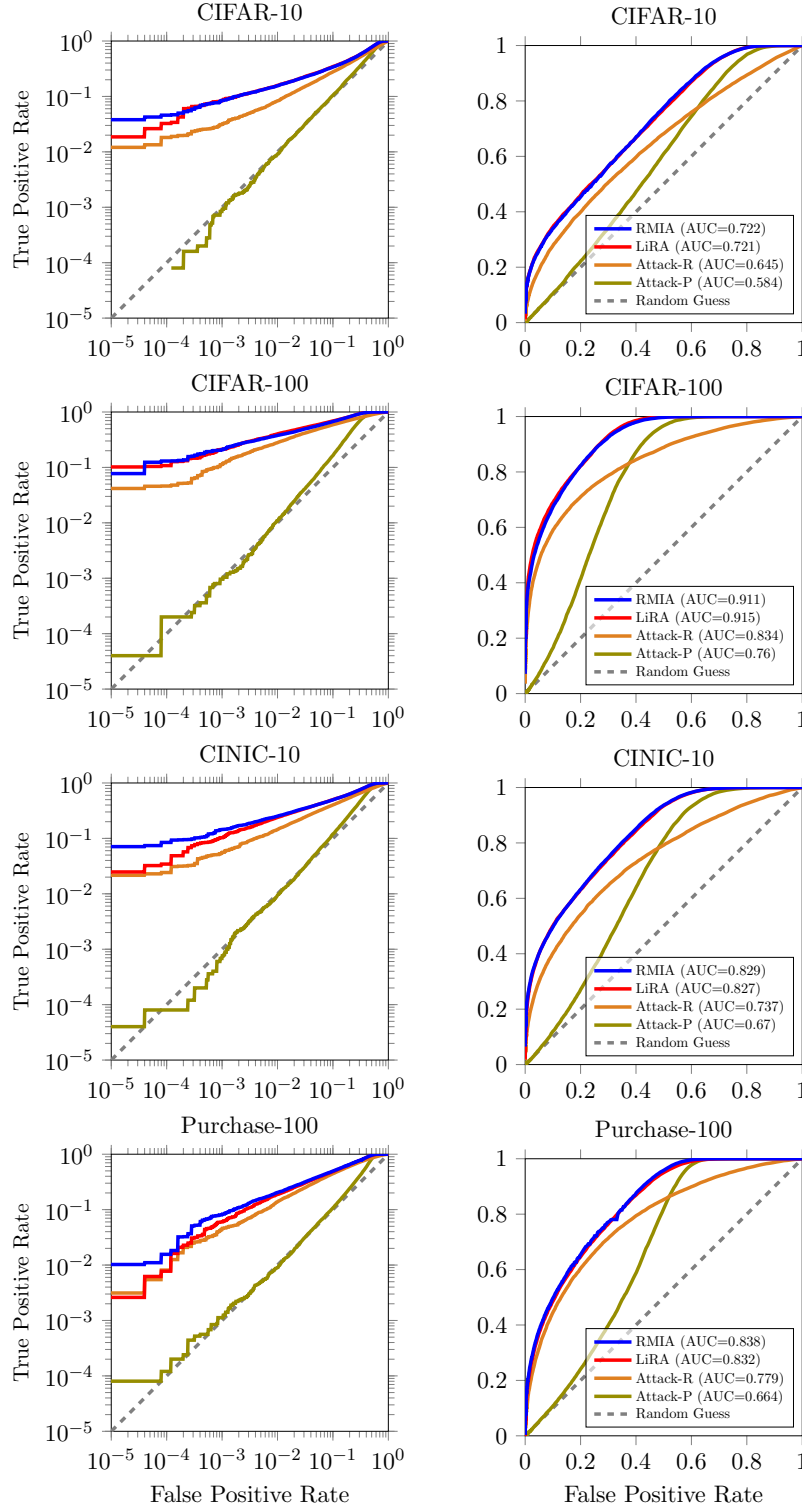


Figure 14: ROC of attacks using models trained on different datasets (ROC's are shown in both log and normal scales). The result is obtained on one random target model. We here use **254** reference models (127 IN, 127 OUT).

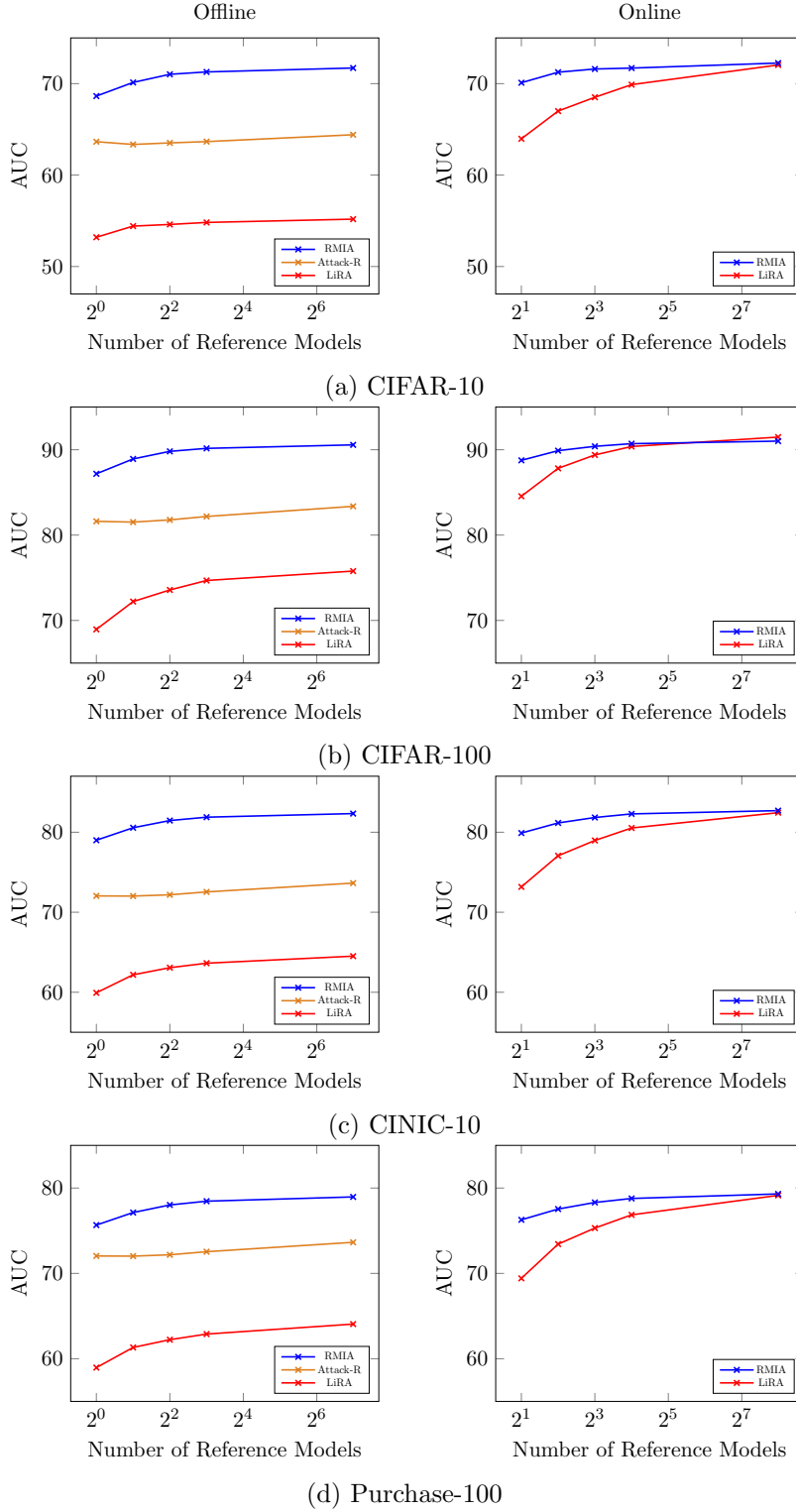


Figure 15: AUC of various attacks obtained with using different number of reference models. The left plots illustrate the results of offline attacks, while the right ones depict the AUC scores obtained by online attacks. For online attacks, half of reference models are OUT and half are IN.

C.2 Robustness of Attacks against Noise and OOD

To evaluate the performance of attacks against OOD test samples, we consider two strategies for generating non-member test queries: incorporating samples from a dataset different from the training dataset and using pure noise. Figure 16 illustrates the ROC curves of three offline attacks using models trained on CIFAR-10. We use 127 reference models (OUT). The ROCs are presented in normal scale to highlight the gap between attacks. To generate OOD samples, we employ samples from CINIC-10 with the same label as CIFAR-10. When using OOD samples as test queries (depicted in the left plot), we observe a substantial performance gap (at least 21% higher AUC) between RMIA and other attacks, with LiRA not performing much better than random guessing. In the case of using noise as non-member test queries (depicted in the right plot), RMIA once again outperforms the other two attacks by at least 61% in terms of AUC, while LiRA falls significantly below the random guess.

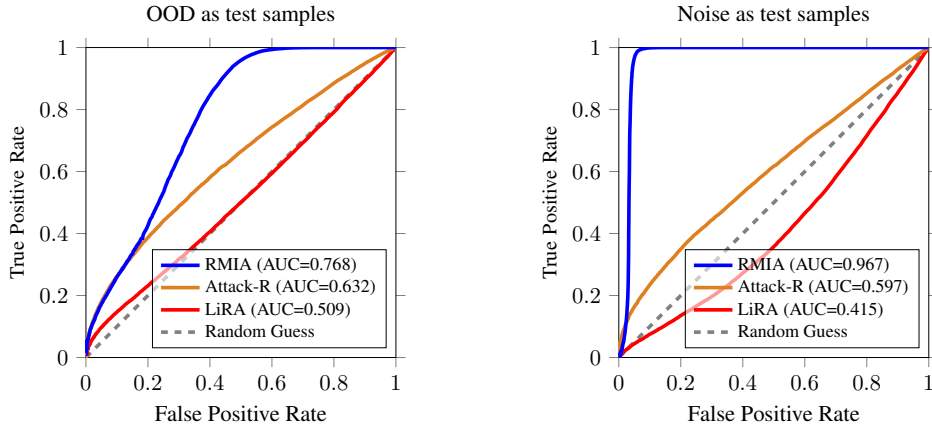


Figure 16: ROC of three offline attacks using models trained on CIFAR-10 when non-member test queries come from a distribution different from the population data π . The result is obtained on one random target model. The left plot uses out-of-distribution (OOD) samples from CINIC-10 (with the same label as CIFAR-10) as non-member test queries, while the right plot uses random noise. We here use 127 reference models (OUT).

C.3 Data Distribution Shift

Table 7 compares the result of attacks when the target models are trained on different datasets than the reference models. More specifically, the target models are trained on CIFAR-10, while the reference models are trained on CINIC-10 (all test queries are from CIFAR-10). We use images with common class labels between two datasets. We here concentrate on offline attacks, as the reference models are trained on a completely different dataset than the target model. We report the results obtained with different number of reference models (1, 2 and 4). The shift in distribution of training data between the target model and the reference models affects the performance of all attacks. Compared with other two attacks, RMIA always obtains a higher AUC (e.g. by up to 25% in comparison with LiRA) and a better TPR at low FPRs.

# Ref Models	Attack	AUC	TPR@FPR	
			0.01%	0.0%
1	Attack-R, [54]	61.41 ± 0.23	0.02	0.01
	LiRA (Offline), [8]	54.48 ± 0.21	0.06	0.01
	RMIA (Offline)	64.84 ± 0.25	0.06	0.02
2	Attack-R, [54]	61.45 ± 0.30	0.03	0.01
	LiRA (Offline), [8]	52.58 ± 0.18	0.01	0.00
	RMIA (Offline)	66.05 ± 0.29	0.13	0.04
4	Attack-R, [54]	61.54 ± 0.30	0.04	0.02
	LiRA (Offline), [8]	55.15 ± 0.25	0.03	0.01
	RMIA (Offline)	66.78 ± 0.32	0.22	0.09

Table 7: Performance of offline attacks when different datasets are used for training target and reference models. Specifically, the target models are trained on **CIFAR-10**, while the reference models are trained on **CINIC-10**. We use different numbers of reference models (1, 2 and 4 OUT models). Results are averaged over 10 random target models.

C.4 Variations in Neural Network Architectures

Figure 17 illustrates the performance of attacks when models are trained with different architectures, including CNN and Wide ResNet (WRN) of various sizes, on CIFAR-10. In this scenario, both target and reference models share the same architecture. RMIA consistently outperforms other attacks across all architectures (e.g. 7.5%-16.8% higher AUC compared with LiRA). Using network architectures with more parameters can lead to increased leakage, as shown by [6].

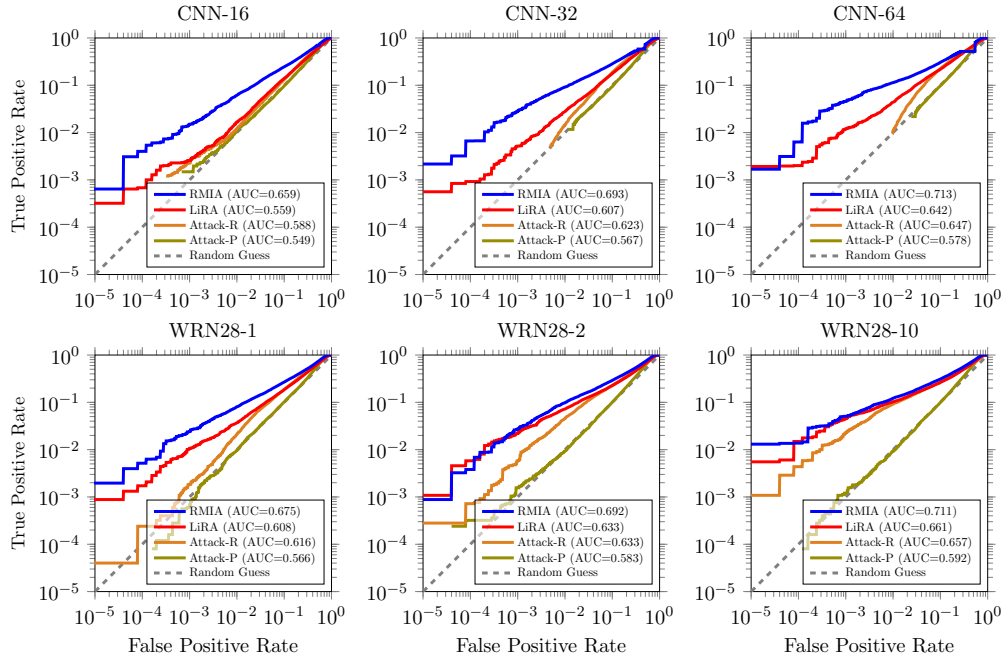


Figure 17: ROC of attacks using different neural network architectures for training models on CIFAR-10. Here, both target and reference models share the same architecture. We use 2 reference models (1 IN, 1 OUT).

Figure 18 presents the performance of attacks when different architectures are used to train reference models, while keeping the structure of the target model fixed as WRN28-2. So, the target and reference models may have different architectures. The optimal performance for both RMIA and LiRA is observed when both target and reference models share similar architectures. However, RMIA outperforms other attacks again, and notably, the performance gap widens under architecture shifts.

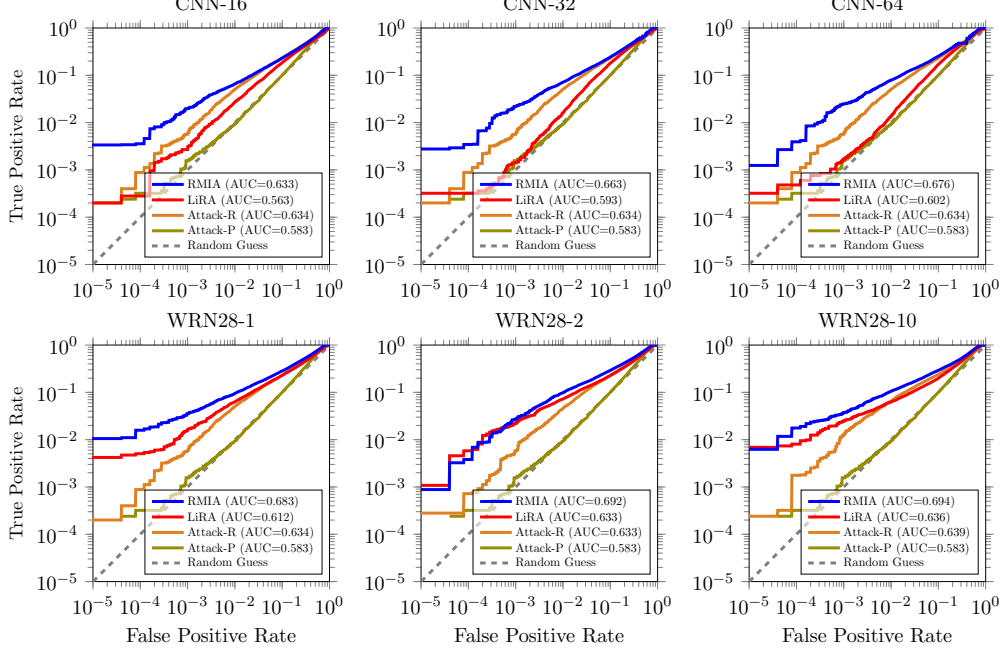


Figure 18: ROC of attacks using different neural network architectures for training reference models on CIFAR-10. The target model is always trained using WRN28-2. We here use 2 reference models (1 IN, 1 OUT).

C.5 Attacking DP-SGD

Differential Privacy (DP) serves as a primary defense mechanism against privacy attacks, including membership inference on machine learning models. It establishes an upper bound on the success of any membership inference attack. Similar to the setting used in [8], we assess the impact of DP-SGD [1] on the performance of various attacks, exploring three combinations of DP-SGD’s noise multiplier and clipping norm parameters across different privacy budgets: 1) for $\epsilon = \infty$, we set the noise multiplier $\sigma = 0.0$ and clipping gradient $C = 10$ (resulting in a test accuracy of 80.53%), 2) for $\epsilon = 6300$, we use $\sigma = 0.2$ and $C = 5$ (resulting in a test accuracy of 73.59%), and 3) for $\epsilon = 26$, we opt $\sigma = 0.8$ and $C = 1$ (yielding a test accuracy of 49.89%). As noted by [8], well-trained models with DP-SGD exhibit membership inference performance close to random guessing. To enhance model memorization, we deliberately flip the label of a small portion (around 2%) of samples in the population before training. Finally, a balanced set of relabeled member and non-member samples is used to evaluate the attacks.

Figure 19 depicts the ROC of attacks when DP-SGD is used to train CNN-32 models on the CIFAR-10 dataset. We employ 4 reference models (2 IN, 2 OUT). Across all three settings,

RMIA outperforms the other three attacks in terms of the obtained AUC. Specifically, in the more relaxed setting (with an infinite budget, zero noise multiplier, and a large clipping gradient), it yields around 3% higher AUC and also a higher TPR at zero FPR than its closest rival. In the other two stringent settings, our attack further enhances its superiority over other attacks concerning AUC (e.g. by at least 6.5% higher AUC than LiRA), although the performance of all attacks tends to converge to random guessing. DP-SGD is shown to be an effective method to mitigate membership inference attacks but comes at the cost of significantly degrading the accuracy of the model.

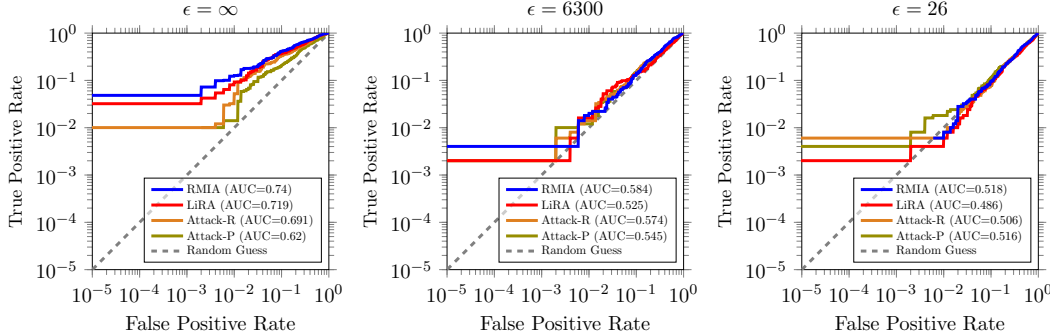


Figure 19: ROC of attacks using DP-SGD for training CNN-32 models on CIFAR-10. We deliberately flip the label of 2% of samples to enhance model memorization. Three distinct privacy budgets, each accompanied by specific settings for DP-SGD parameters, are used: $\epsilon = \infty$ (left plot), $\epsilon = 6300$ (middle plot), and $\epsilon = 26$ (right plot). Here, we use 4 reference models (2 IN, 2 OUT).

C.6 Performance of Attacks on Models Trained with other ML Algorithms

While the majority of contemporary machine learning (ML) models rely on neural networks, understanding how attacks generalize in the presence of other machine learning algorithms is intriguing. Although it is beyond the scope of this paper to comprehensively analyze attacks across a wide range of ML algorithms on various datasets, we conduct a simple experiment to study their impact by training models with a Gradient Boosting Decision Tree (GBDT) algorithm. Figure 20 illustrates the ROC of attacks when GBDT (with three different max depths) is employed to train models on our non-image dataset, i.e. Purchase-100. The hyperparameters of GBDT are set as `n_estimators=250`, `lr=0.1` and `subsample=0.2`, yielding a test accuracy of around 53%. For this experiment, we use two reference models (1 IN, 1 OUT). Since the output of GBDT is the prediction probability (not logit), we use this probability as the input signal for all attacks. To compute the rescaled-logit signal for LiRA, we use $\log(\frac{p}{1-p})$, where p is the output probability. The TPR obtained by our attack consistently outperforms all other attacks, particularly by an order of magnitude at zero FPR.

C.7 MIA Score Comparison between Attacks

Figure 21 illustrates the distribution of MIA scores obtained from various attacks for a set of test samples. In generating these distributions, we apply the attacks to 254 target models, with each sample being a member to half of them and a non-member to the other half. The attacks

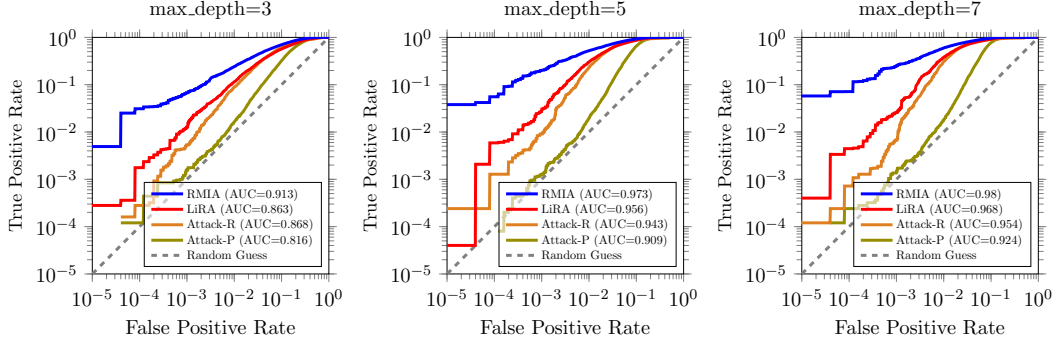


Figure 20: ROC of attacks on models trained with Gradient Boosted Decision Tree (GBDT) on the Purchase-100 dataset. Three different values of max depth parameter are used in GBDT. The test accuracy of models is around 53%. We use 2 reference models (1 IN, 1 OUT). In LiRA [8], we use the output probability p to compute the rescaled-logit signal as $\log(\frac{p}{1-p})$. In other attacks, we use the output probability as the input signal of attacks.

are conducted using 127 OUT reference models trained on CIFAR-10. It is evident that the MIA score produced by RMIA contributes to a more distinct separation between members and non-members across all samples, as member scores tend to concentrate in the right part of the plot.

To better understand the difference between the performance of our attack with others' (specially when focusing on low FPRs), we compare the MIA score of member and non-member samples obtained in RMIA and other attacks. Figure 22 displays RMIA scores versus LiRA scores in two scenarios: one using only 1 reference model (shown on the left) and another using 4 reference models (shown on the right). With just 1 reference model, RMIA provides clearer differentiation between numerous member and non-member samples, as it assigns distinct MIA scores in the $[0, 1]$ range, separating many members on the right side and non-members on the left side. In contrast, LiRA scores are more concentrated towards the upper side of the plot, lacking a distinct separation between member and non-member scores. When employing more reference models, we observe a higher degree of correlation between the scores of the two attacks.

Similarly, Figure 23 shows RMIA scores compared to Attack-R scores in the same two scenarios: using only 1 reference model (shown on the left) and using 4 reference models (shown on the right). For both scenarios, RMIA can better separate members from non-members via assigning distinct MIA scores to them (member scores apparently tend to be larger than non-member scores for lots of samples). In contrast, there is no such clear distinction in Attack-R.

We finally show RMIA scores versus Attack-P scores in Figure 24. In this experiment, we only use 1 reference model (OUT) for RMIA, because Attack-P does not work with reference models. As opposed to RMIA, Attack-P clearly fails to provide a good separation between member and non-member scores.

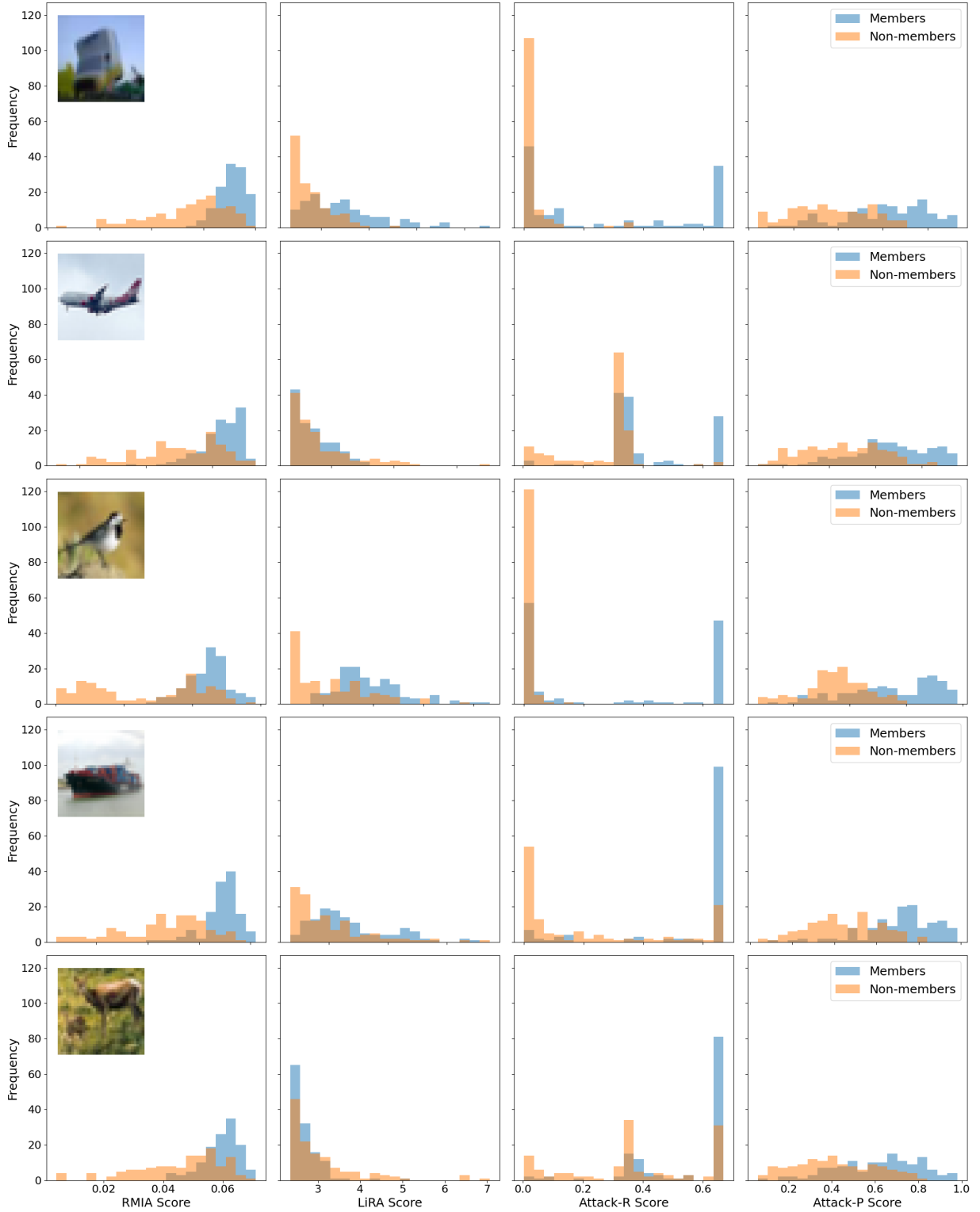


Figure 21: Distribution of MIA scores obtained from different attacks for some test sample. We calculate the MIA score of each sample across 254 target models where half of them are IN models, and the remaining half are OUT models. To perform attacks, we use 127 reference models (OUT), trained on CIFAR-10.

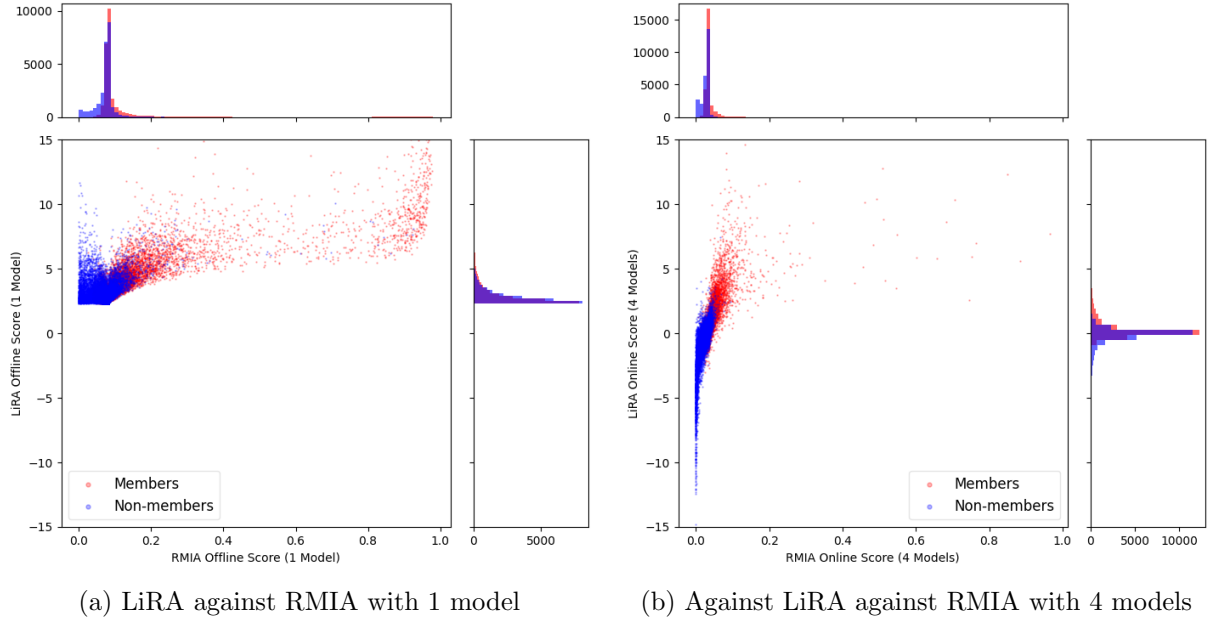


Figure 22: MIA score comparison between RMIA and LiRA [8] over all member and non-member samples of a random target model. The left plot is obtained when only 1 reference model (OUT) is used, while the right plot uses 4 reference models (2 IN and 2 OUT). In both plots, the x-axis represents RMIA scores, while the y-axis depicts LiRA scores.

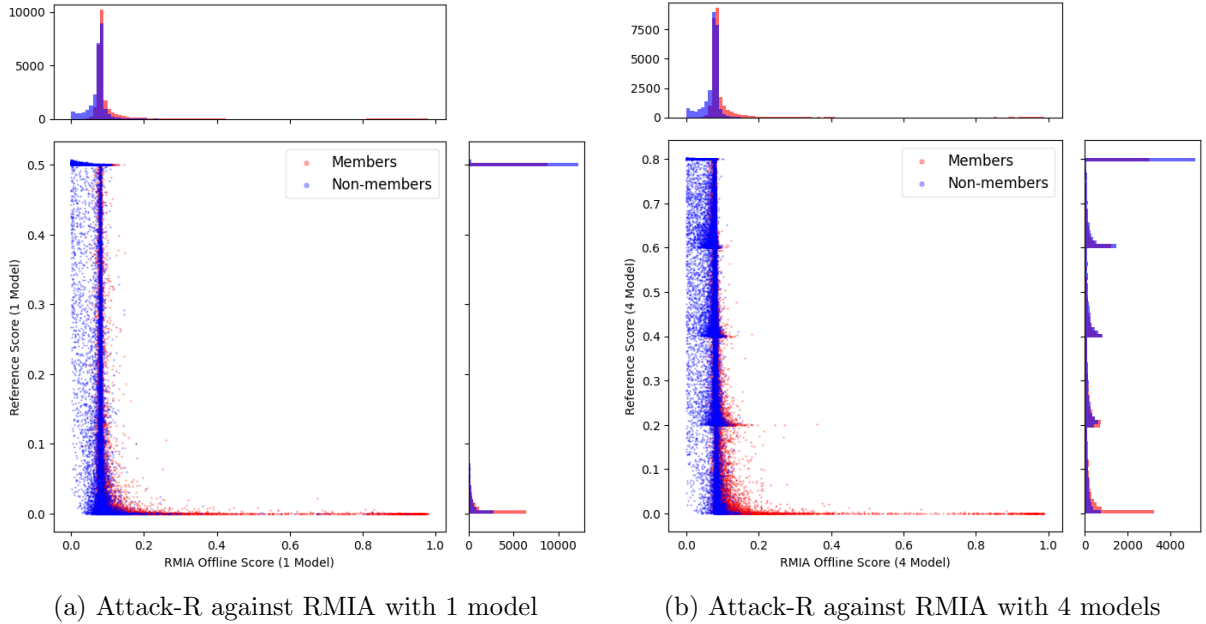


Figure 23: MIA score comparison between RMIA and Attack-R [54] over all member and non-member samples of a random target model. The left plot is obtained when only 1 reference model (OUT) is used, while the right plot uses 4 models (OUT). In both plots, the x-axis represents RMIA scores, while the y-axis depicts Attack-R scores.

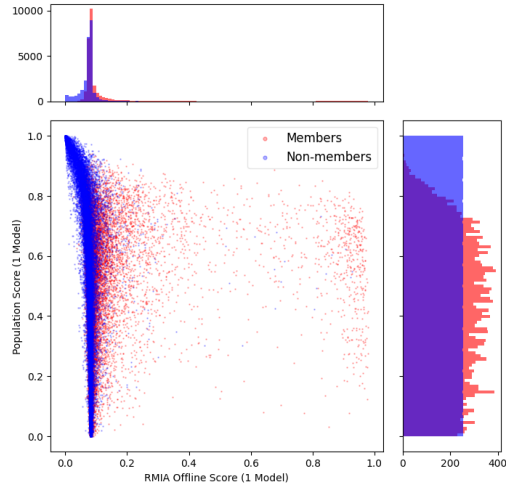


Figure 24: MIA score comparison between RMIA and Attack-P [54] obtained for a random target model. The x-axis represents RMIA scores, while the y-axis depicts Attack-P scores. RMIA results are computed using only 1 reference model (OUT).